

Identification of optimal drug combinations targeting cellular networks: integrating phospho-proteomics and computational network analysis

Authors and Affiliations

Sergio Iadevaia, Yiling Lu, Fabiana C. Morales, Gordon B. Mills, and Prahlad T. Ram
Department of Systems Biology, The University of Texas M. D. Anderson Cancer Center,
Houston, Texas, United States of America

Contents

- S1. IGFR signaling network in the MDA-MB231 breast cancer cell line
 - S1a. References for molecule interactions defining the IGFR signaling network topology*
 - S1b. Formulation of the mass-action ODE model*
 - S2. Computational procedures
 - S3. Dose response of the MDA-MB231 cell line to treatment with drug inhibitors
 - S4. Reduced IGFR signaling network in the MDA-MB231 breast cancer cell line
 - S5. Comparison between dynamics predicted by the original and reduced ODE models
 - S6. Perturbing IGFR signaling dynamics using drug inhibitors
- Supplemental files
- Supplemental tables
- References

Supplemental Material S1. IGFR signaling network in the MDA-MB231 breast cancer cell line

The topologic features of cell signaling networks at the elementary reaction level are largely unknown. Consensus maps are typically structured as sets of reactions that define the simplified mechanisms of activation and inhibition of relevant proteins. To reconstruct the IGFR signaling network in the MDA-MB231 cell line, we overlaid consensus maps onto RPPA data and obtained the following set of chemical reactions:

1. IGF binding to IGF receptor



2. IGF receptor auto-phosphorylation



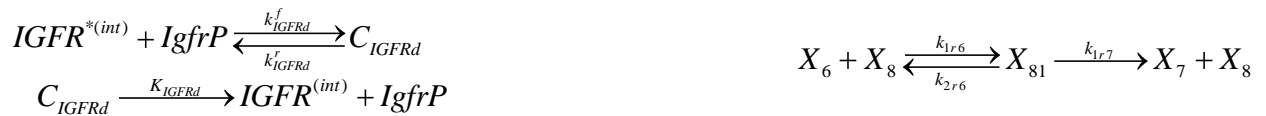
3. IGF receptor internalization



4. Dissociation of activated IGF receptor



5. IGF receptor de-phosphorylation



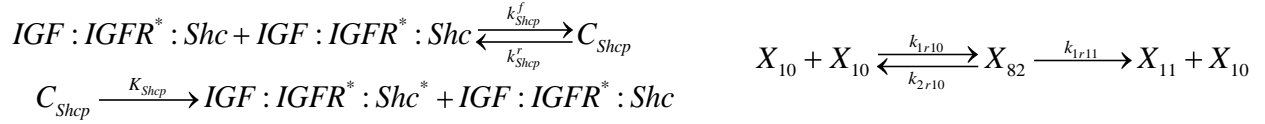
6. IGF receptor re-integration



7. Binding of Shc to IGF receptor



8. Shc phosphorylation



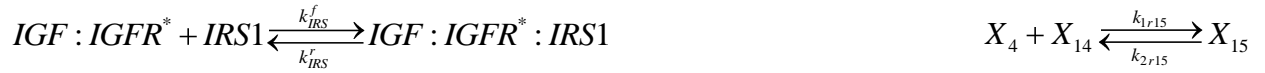
9. Dissociation of p-Shc from activated IGF receptor



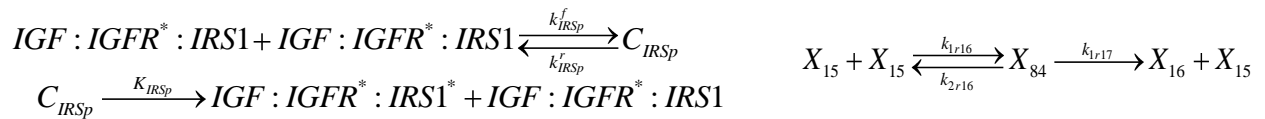
10. Shc de-phosphorylation



11. Binding of IRS1 to activated IGF receptor



12. IRS1 phosphorylation



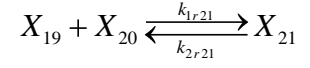
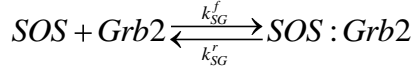
13. Dissociation of p-IRS1 from activated IGF receptor



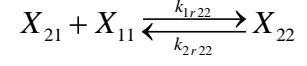
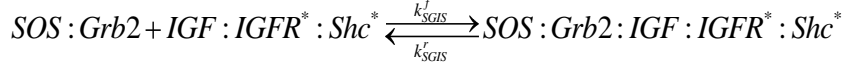
14. IRS1 de-phosphorylation



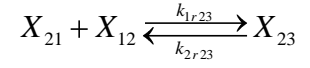
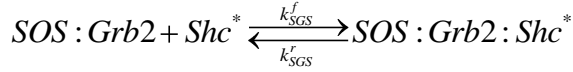
15. SOS-Grb2 binding



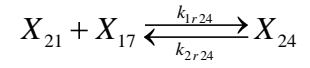
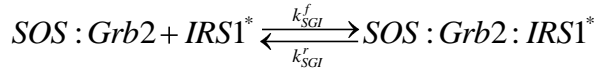
16. SOS-Grb2-Shc-IGFR binding



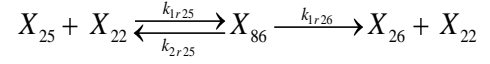
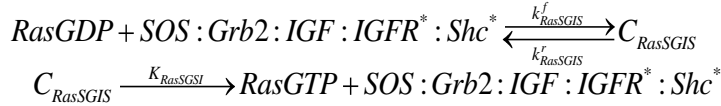
17. SOS-Grb2-Shc binding



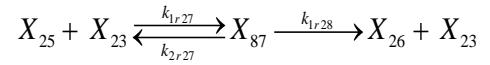
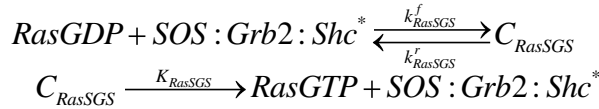
18. SOS-Grb2-IRS1 binding



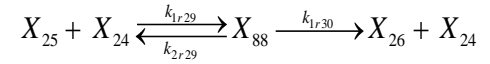
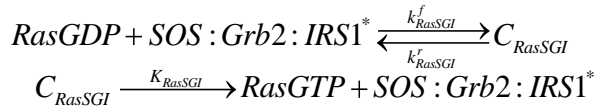
19. RasGTP activation by SGIS



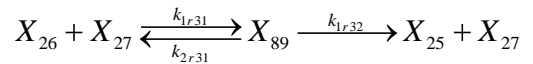
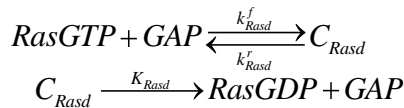
20. RasGTP activation by SGS



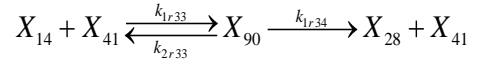
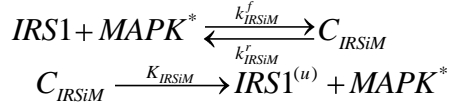
21. RasGTP activation by SGI



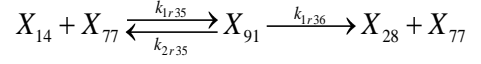
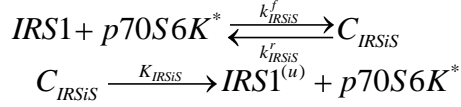
22. Ras de-activation



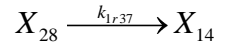
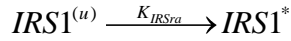
23. IRS1 inhibition by MAPK



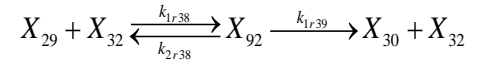
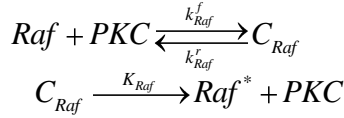
24. IRS1 inhibition by p70S6K



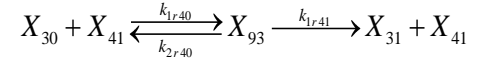
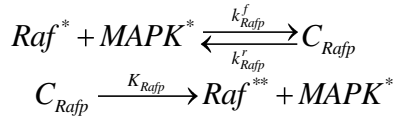
25. IRS1 re-activation



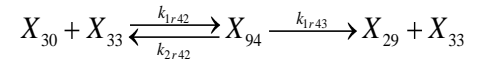
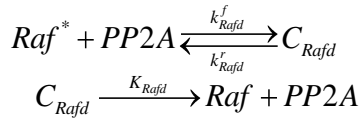
26. Raf activation by PKC



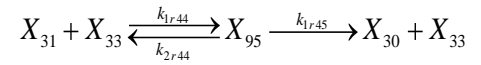
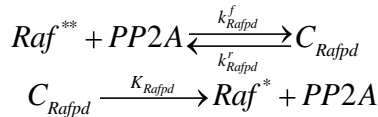
27. Raf^{*} activation by MAPK



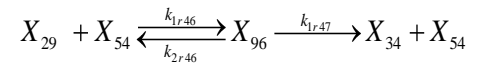
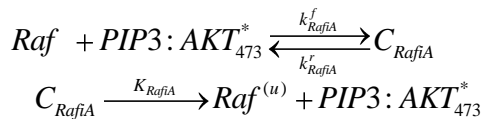
28. Raf^{*} de-activation by PP2A



29. Raf^{**} de-activation by PP2A



30. Raf inhibition by AKT



31. Raf re-activation



32. Ras-Raf activation



33. MEK activation by Ras-Raf



34. MEK* activation by Ras-Raf



35. MEK* de-activation by PP2A



36. MEK** de-activation by PP2A



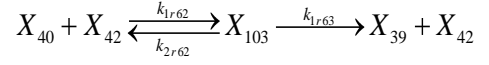
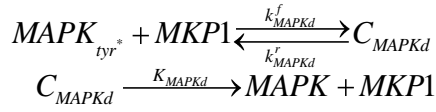
37. MAPK tyrosine activation by MEK**



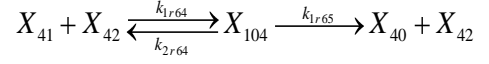
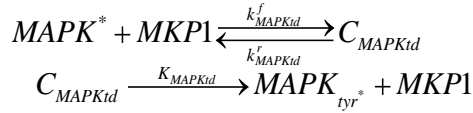
38. MAPK activation by MEK**



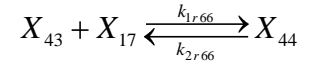
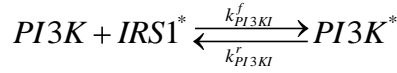
39. MAPK tyrosine inactivation by MKP1



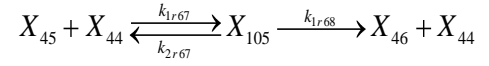
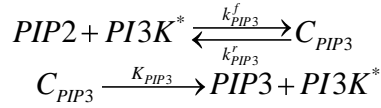
40. MAPK inactivation by MKP1



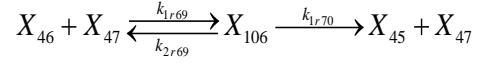
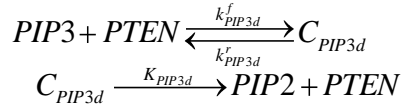
41. PI3K activation by IRS1



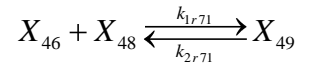
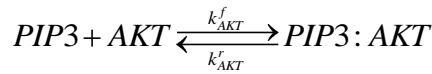
42. PIP3 formation



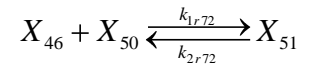
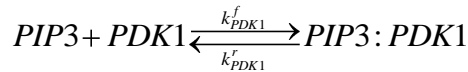
43. PIP3 hydrolysis by PTEN



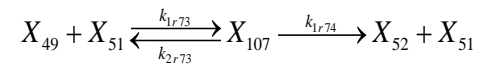
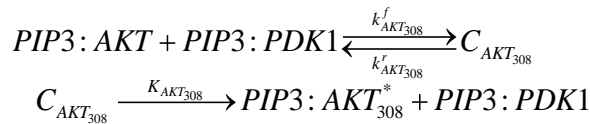
44. AKT attachment to membrane



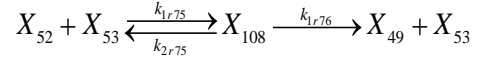
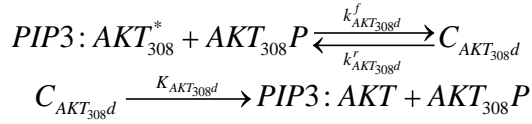
45. PDK1 attachment to membrane



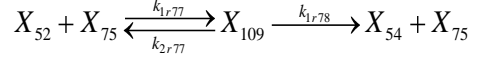
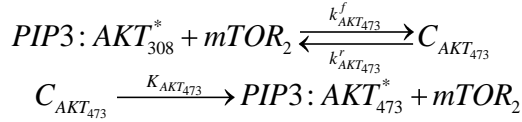
46. Activation of AKT₃₀₈ by PDK1



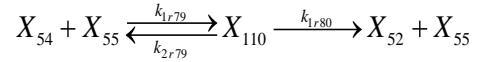
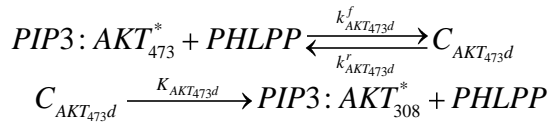
47. AKT₃₀₈ de-activation



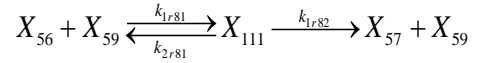
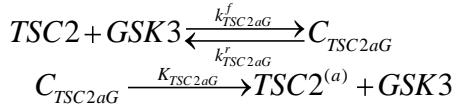
48. AKT₄₇₃ activation by mTOR₂



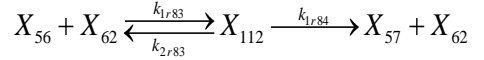
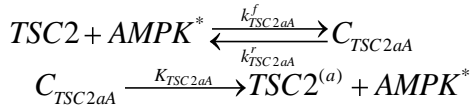
49. De-activation of AKT₄₇₃ by PHLPP



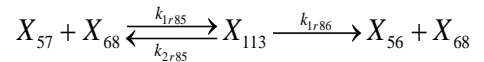
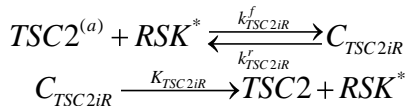
50. TSC2 activation by GSK3



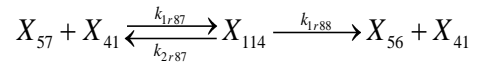
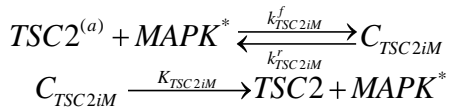
51. TSC2 activation by AMPK



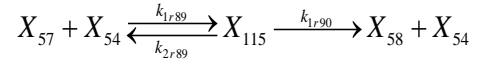
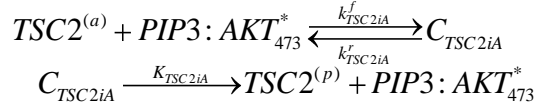
52. TSC2 inactivation by RSK



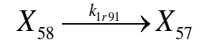
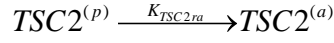
53. TSC2 inactivation by MAPK



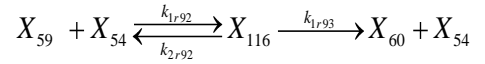
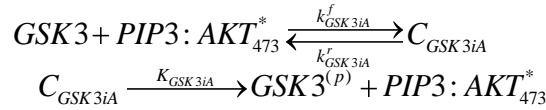
54. TSC2 inactivation by AKT



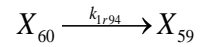
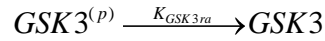
55. TSC2 re-activation



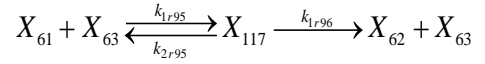
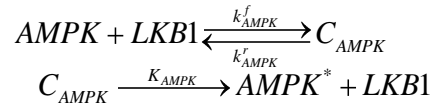
56. GSK3 inhibition by AKT



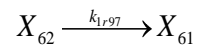
57. GSK3 re-activation



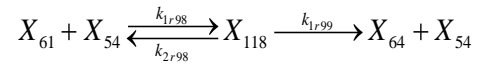
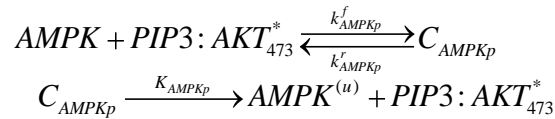
58. AMPK activation by LKB1



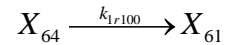
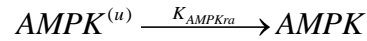
59. AMPK de-activation



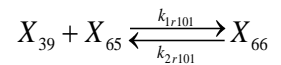
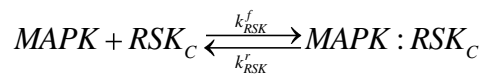
60. AMPK inhibition by AKT



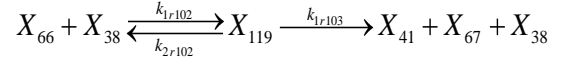
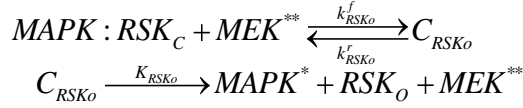
61. AMPK re-activation



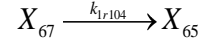
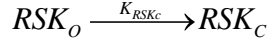
62. MAPK-RSK complex formation



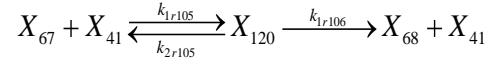
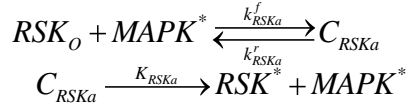
63. RSK kinase opening



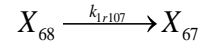
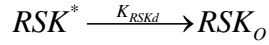
64. RSK kinase closing



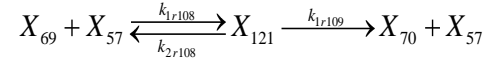
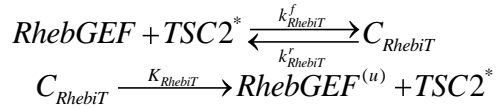
65. RSK activation by MAPK



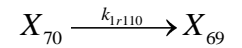
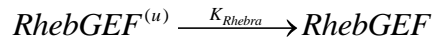
66. RSK de-activation



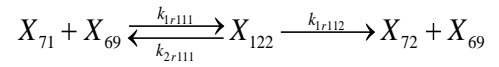
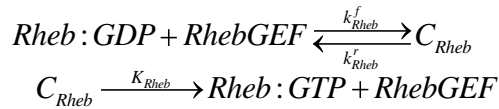
67. Rheb de-activation by TSC2



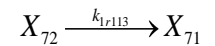
68. Rheb re-activation



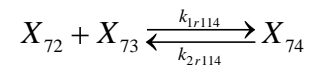
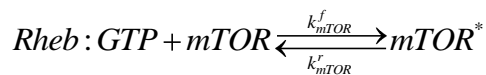
69. GTP loading by Rheb



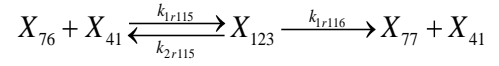
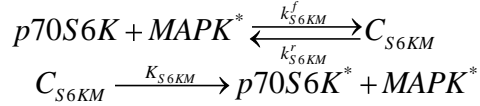
70. Rheb de-activation



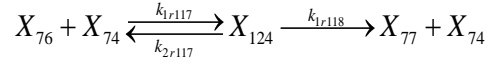
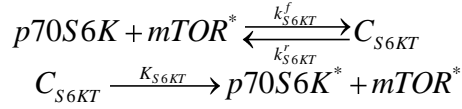
71. mTOR formation



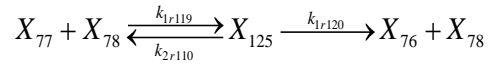
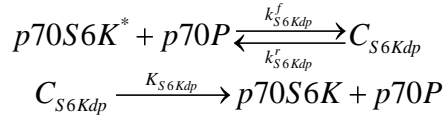
72. p70S6K activation by MAPK



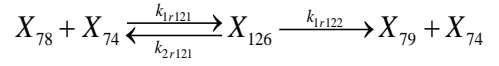
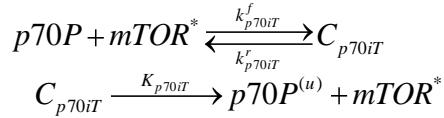
73. p70S6K activation by mTOR



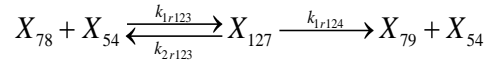
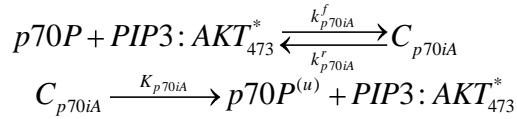
74. De-activation of p70S6K



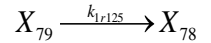
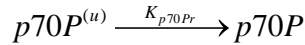
75. p70P inhibition by mTOR



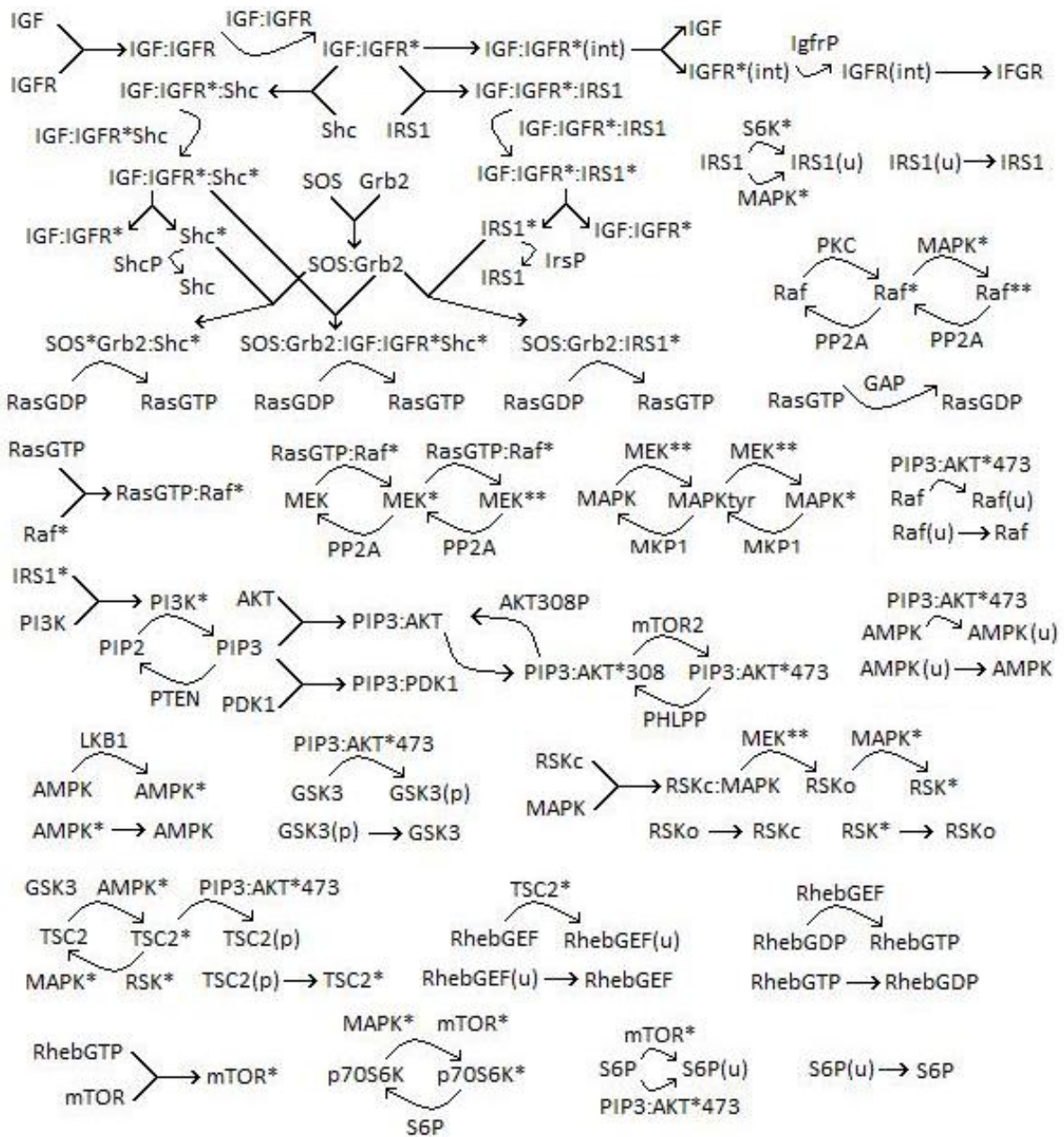
76. p70P inhibition by AKT



77. p70P re-activation



Supplemental Figure 1 summarizes the reconstructed IGFR signaling network. The reconstructed IGFR signaling network included 6 feed-forward and 3 feed-back loops, and was comprised of 127 species involved into 77 chemical reactions.



Supplemental Figure 1. The signaling network through the insulin-like growth factor (IGF-1) receptor tyrosine kinase in the K-Ras and B-Raf mutant MDA-MB231 cell line. Signal transduction is originated when the IGF-1 ligand complexes with IGF receptor (IGFR) and triggers autophosphorylation of the IGFR tyrosine kinase. Phosphorylated IGFR propagates the signal downstream through the MAPK and PI3K pathways activation and leads to MAPK and AKT phosphorylation (1, 2). The signals from the MAPK and PI3K cascades are routed to the mTOR pathways via TSC2 inactivation (3). Phosphorylated mTOR activates p70S6K, which can downregulate IRS-1 levels through a negative feedback loop (4). In the absence of IGF stimulation, genetic mutations encoded in the MDA-MB231 cell line lead to high basal activity of Ras and Raf, which drives constitutive activation of the MAPK pathway.

Supplemental Material S1a. References for molecule interactions defining the IGFR signaling network topology

Reactions 1-6 describe the mechanisms of IGFR phosphorylation and internalization (5). Reactions 7-10 and 11-14 account for Shc and IRS-1 activation, respectively (5). Reactions 15-22 model the GDP/GTP exchange on Ras that is catalyzed by Shc-Grb2-SOS, IGFR-Shc-Grb2-SOS, and IRS-Grb2-SOS (5). Reactions 23-25 model IRS-1-mediated inhibition by MAPK (6) and p70S6K (4). Because the mechanisms of IRS-1 inhibition are unknown, we treated these interactions as black boxes and hypothesized that MAPK and p70S6K do not decrease the level of IRS-1 phosphorylation but render it unavailable (subscript u) to activate downstream effectors. Reactions 26-29 and 32-40 describe MAPK activation via Raf and MEK (7). Reactions 28-29, 35-36, and 39-40 describe the effect of transcriptional feedback regulations and account for changes in the immediate early genes PP2A and MKP1 (7). Reactions 30-31 account for AKT-mediated inactivation of Raf (8). Reactions 41-49 describe PI3K-mediated activation of AKT, including AKT downregulation triggered by PTEN (5). Reactions 50-55 model TSC2 activation mediated by AMPK and GSK3 (9) and TSC2 inactivation driven by AKT (5), MAPK (10) and RSK (11). Reactions 56-57 and 60-61 describe AMPK (12) and GSK3 (5) inactivation by AKT, and reactions 58-59 account for LKB1-mediated activation of AMPK (5). Reactions 62-66 describe RSK activation by MAPK (13). Reactions 67-71 model mTOR activation mediated by Rheb (5). Finally, reactions 72-74 describe direct activation of p70S6K driven by MAPK (14) and mTOR (15), and reactions 75-77 account for modular activation of p70S6K mediated by mTOR (15) and AKT (16).

Supplemental Material S2a. Formulation of the mass-action ODE model formulation

Assuming that the kinetics of the reconstructed network obeyed the law of mass-action, we derived a system of 127 coupled ODEs (original model) with 313 unknown model parameters, 186 of which were signaling rate constants and the remaining 127 of which were initial concentrations:

$$\frac{dx_1}{dt} = -k_{1r1}x_1x_2 + k_{2r1}x_3 + k_{1r5}x_5 \quad (\text{O.1})$$

$$\frac{dx_2}{dt} = -k_{1r1}x_1x_2 + k_{2r1}x_3 + k_{1r8}x_7 \quad (\text{O.2})$$

$$\frac{dx_3}{dt} = k_{1r1}x_1x_2 - k_{2r1}x_3 - 2k_{1r2}x_3^2 + 2k_{2r2}x_{30} + k_{1r3}x_{80} \quad (\text{O.3})$$

$$\begin{aligned} \frac{dx_4}{dt} = & k_{1r3}x_{80} - k_{1r4}x_4 - k_{1r9}x_4x_9 + k_{2r9}x_{10} + k_{1r12}x_{11} - k_{1r15}x_4x_{14} + \\ & + k_{2r15}x_{15} + k_{1r18}x_{16} \end{aligned} \quad (\text{O.4})$$

$$\frac{dx_5}{dt} = k_{1r4}x_4 - k_{1r5}x_5 \quad (\text{O.5})$$

$$\frac{dx_6}{dt} = k_{1r5}x_5 - k_{1r6}x_6x_8 + k_{2r6}x_{81} \quad (\text{O.6})$$

$$\frac{dx_7}{dt} = k_{1r7}x_{81} - k_{1r8}x_7 \quad (\text{O.7})$$

$$\frac{dx_8}{dt} = -k_{1r6}x_6x_8 + k_{2r6}x_{81} + k_{1r7}x_{81} \quad (\text{O.8})$$

$$\frac{dx_9}{dt} = -k_{1r9}x_4x_9 + k_{2r9}x_{10} + k_{1r14}x_{83} \quad (\text{O.9})$$

$$\frac{dx_{10}}{dt} = k_{1r9}x_4x_9 - k_{2r9}x_{10} - 2k_{1r10}x_{10}^2 + 2k_{2r10}x_{82} + k_{1r11}x_{82} \quad (\text{O.10})$$

$$\frac{dx_{11}}{dt} = k_{1r11}x_{82} - k_{1r12}x_{11} - k_{1r22}x_{21}x_{11} + k_{2r22}x_{22} \quad (\text{O.11})$$

$$\frac{dx_{12}}{dt} = k_{1r12}x_{11} - k_{1r13}x_{12}x_{13} + k_{2r13}x_{83} - k_{1r23}x_{21}x_{12} + k_{2r23}x_{23} \quad (\text{O.12})$$

$$\frac{dx_{13}}{dt} = -k_{1r13}x_{12}x_{13} + k_{2r13}x_{83} + k_{1r14}x_{83} \quad (\text{O.13})$$

$$\begin{aligned} \frac{dx_{14}}{dt} = & -k_{1r15}x_4x_{14} + k_{2r15}x_{15} + k_{1r20}x_{85} - k_{1r33}x_{14}x_{41} + k_{2r33}x_{90} + \\ & -k_{1r35}x_{14}x_{77} + k_{2r35}x_{91} + k_{1r37}x_{28} \end{aligned} \quad (\text{O.14})$$

$$\frac{dx_{15}}{dt} = k_{1r15}x_4x_{14} - k_{2r15}x_{15} - 2k_{1r16}x_{15}^2 + 2k_{2r16}x_{84} + k_{1r17}x_{84} \quad (\text{O.15})$$

$$\frac{dx_{16}}{dt} = k_{1r17}x_{84} - k_{1r18}x_{16} \quad (\text{O.16})$$

$$\begin{aligned} \frac{dx_{17}}{dt} = & k_{1r18}x_{16} - k_{1r19}x_{17}x_{18} + k_{2r19}x_{85} - k_{1r24}x_{21}x_{17} + k_{2r24}x_{24} + \\ & -k_{1r66}x_{43}x_{17} + k_{2r66}x_{44} \end{aligned} \quad (\text{O.17})$$

$$\frac{dx_{18}}{dt} = -k_{1r19}x_{17}x_{18} + k_{2r19}x_{85} + k_{1r20}x_{85} \quad (\text{O.18})$$

$$\frac{dx_{19}}{dt} = -k_{1r21}x_{19}x_{20} + k_{2r21}x_{21} \quad (\text{O.19})$$

$$\frac{dx_{20}}{dt} = -k_{1r21}x_{19}x_{20} + k_{2r21}x_{21} \quad (\text{O.20})$$

$$\begin{aligned} \frac{dx_{21}}{dt} = & k_{1r21}x_{19}x_{20} - k_{2r21}x_{21} - k_{1r22}x_{21}x_{11} + k_{2r22}x_{22} - k_{1r23}x_{21}x_{12} + \\ & + k_{2r23}x_{23} - k_{1r24}x_{21}x_{17} + k_{2r24}x_{24} \end{aligned} \quad (\text{O.21})$$

$$\frac{dx_{22}}{dt} = k_{1r22}x_{21}x_{11} - k_{2r22}x_{22} - k_{1r25}x_{25}x_{22} + k_{2r25}x_{86} + k_{1r26}x_{86} \quad (\text{O.22})$$

$$\frac{dx_{23}}{dt} = k_{1r23}x_{21}x_{12} - k_{2r23}x_{23} - k_{1r27}x_{25}x_{23} + k_{2r27}x_{87} + k_{1r28}x_{87} \quad (\text{O.23})$$

$$\frac{dx_{24}}{dt} = k_{1r24}x_{21}x_{17} - k_{2r24}x_{24} - k_{1r29}x_{25}x_{24} + k_{2r29}x_{88} + k_{1r30}x_{88} \quad (\text{O.24})$$

$$\begin{aligned} \frac{dx_{25}}{dt} = & -k_{1r25}x_{25}x_{22} + k_{2r25}x_{86} - k_{1r27}x_{25}x_{23} + k_{2r27}x_{87} + \\ & -k_{1r29}x_{25}x_{24} + k_{2r29}x_{88} + k_{1r32}x_{89} \end{aligned} \quad (\text{O.25})$$

$$\begin{aligned} \frac{dx_{26}}{dt} = & k_{1r26}x_{86} + k_{1r28}x_{87} + k_{1r30}x_{88} - k_{1r31}x_{26}x_{27} + k_{2r31}x_{89} + \\ & -k_{1r49}x_{26}x_{30} + k_{2r49}x_{35} \end{aligned} \quad (\text{O.26})$$

$$\frac{dx_{27}}{dt} = -k_{1r31}x_{26}x_{27} + k_{2r31}x_{89} + k_{1r32}x_{89} \quad (\text{O.27})$$

$$\frac{dx_{28}}{dt} = k_{1r34}x_{90} + k_{1r36}x_{91} - k_{1r37}x_{28} \quad (\text{O.28})$$

$$\frac{dx_{29}}{dt} = -k_{1r38}x_{29}x_{32} + k_{2r38}x_{92} + k_{1r43}x_{94} - k_{1r46}x_{29}x_{54} + k_{2r46}x_{96} + k_{1r48}x_{34} \quad (\text{O.29})$$

$$\begin{aligned} \frac{dx_{30}}{dt} = & k_{1r39}x_{92} - k_{1r40}x_{30}x_{41} + k_{2r40}x_{93} - k_{1r42}x_{30}x_{33} + k_{2r42}x_{94} + \\ & + k_{1r45}x_{95} - k_{1r49}x_{26}x_{30} + k_{2r49}x_{35} \end{aligned} \quad (\text{O.30})$$

$$\frac{dx_{31}}{dt} = k_{1r41}x_{93} - k_{1r44}x_{31}x_{33} + k_{2r44}x_{95} \quad (\text{O.31})$$

$$\frac{dx_{32}}{dt} = -k_{1r38}x_{29}x_{32} + k_{2r38}x_{92} + k_{1r39}x_{92} \quad (\text{O.32})$$

$$\begin{aligned} \frac{dx_{33}}{dt} = & -k_{1r42}x_{30}x_{33} + k_{2r42}x_{94} + k_{1r43}x_{94} - k_{1r44}x_{31}x_{33} + k_{2r44}x_{95} + \\ & + k_{1r45}x_{95} - k_{1r54}x_{37}x_{33} + k_{2r54}x_{99} + k_{1r55}x_{99} - k_{1r56}x_{38}x_{33} + k_{2r56}x_{100} + k_{1r57}x_{100} \end{aligned} \quad (\text{O.33})$$

$$\frac{dx_{34}}{dt} = k_{1r47}x_{96} - k_{1r48}x_{34} \quad (\text{O.34})$$

$$\begin{aligned} \frac{dx_{35}}{dt} = & k_{1r49}x_{26}x_{30} - k_{2r49}x_{35} - k_{1r50}x_{36}x_{35} + k_{2r50}x_{97} + k_{1r51}x_{97} + \\ & -k_{1r52}x_{37}x_{35} + k_{2r52}x_{98} + k_{1r53}x_{98} \end{aligned} \quad (\text{O.35})$$

$$\frac{dx_{36}}{dt} = -k_{1r50}x_{36}x_{35} + k_{2r50}x_{97} + k_{1r55}x_{99} \quad (\text{O.36})$$

$$\frac{dx_{37}}{dt} = k_{1r51}x_{97} - k_{1r52}x_{37}x_{35} + k_{2r52}x_{98} - k_{1r54}x_{37}x_{33} + k_{2r54}x_{99} + k_{1r57}x_{100} \quad (\text{O.37})$$

$$\begin{aligned} \frac{dx_{38}}{dt} = & k_{1r53}x_{98} - k_{1r56}x_{38}x_{33} + k_{2r56}x_{100} - k_{1r58}x_{39}x_{38} + k_{2r58}x_{101} + k_{1r59}x_{101} + \\ & - k_{1r60}x_{40}x_{38} + k_{2r60}x_{102} + k_{1r61}x_{102} - k_{1r102}x_{66}x_{38} + k_{2r102}x_{119} + k_{1r103}x_{119} \end{aligned} \quad (\text{O.38})$$

$$\frac{dx_{39}}{dt} = -k_{1r58}x_{39}x_{38} + k_{2r58}x_{101} + k_{1r63}x_{103} - k_{1r101}x_{39}x_{65} + k_{2r101}x_{66} \quad (\text{O.39})$$

$$\frac{dx_{40}}{dt} = k_{1r59}x_{101} - k_{1r60}x_{40}x_{38} + k_{2r60}x_{102} - k_{1r62}x_{40}x_{42} + k_{2r62}x_{103} + k_{1r65}x_{104} \quad (\text{O.40})$$

$$\begin{aligned} \frac{dx_{41}}{dt} = & -k_{1r33}x_{14}x_{41} + k_{2r33}x_{90} + k_{1r34}x_{90} - k_{1r40}x_{30}x_{41} + k_{2r40}x_{93} + k_{1r41}x_{93} + \\ & + k_{1r61}x_{102} - k_{1r64}x_{41}x_{42} + k_{2r64}x_{104} - k_{1r87}x_{57}x_{41} + k_{2r87}x_{114} + k_{1r88}x_{114} + \\ & + k_{1r103}x_{119} - k_{1r105}x_{67}x_{41} + k_{2r105}x_{120} + k_{1r106}x_{120} - k_{1r115}x_{76}x_{41} + \\ & + k_{2r115}x_{123} + k_{1r116}x_{123} \end{aligned} \quad (\text{O.41})$$

$$\frac{dx_{42}}{dt} = -k_{1r62}x_{40}x_{42} + k_{2r62}x_{103} + k_{1r63}x_{103} - k_{1r64}x_{41}x_{42} + k_{2r64}x_{104} + k_{1r65}x_{104} \quad (\text{O.42})$$

$$\frac{dx_{43}}{dt} = -k_{1r66}x_{43}x_{17} - k_{2r66}x_{44} \quad (\text{O.43})$$

$$\frac{dx_{44}}{dt} = k_{1r66}x_{43}x_{17} - k_{2r66}x_{44} - k_{1r67}x_{45}x_{44} + k_{2r67}x_{105} + k_{1r68}x_{105} \quad (\text{O.44})$$

$$\frac{dx_{45}}{dt} = -k_{1r67}x_{45}x_{44} + k_{2r67}x_{105} + k_{1r70}x_{106} \quad (\text{O.45})$$

$$\begin{aligned} \frac{dx_{46}}{dt} = & k_{1r68}x_{105} - k_{1r69}x_{46}x_{47} + k_{2r69}x_{106} - k_{1r71}x_{46}x_{48} + k_{2r71}x_{49} + \\ & - k_{1r72}x_{46}x_{50} + k_{2r72}x_{51} \end{aligned} \quad (\text{O.46})$$

$$\frac{dx_{47}}{dt} = -k_{1r69}x_{46}x_{47} + k_{2r69}x_{106} + k_{1r70}x_{106} \quad (\text{O.47})$$

$$\frac{dx_{48}}{dt} = -k_{1r71}x_{46}x_{48} + k_{2r71}x_{49} \quad (\text{O.48})$$

$$\frac{dx_{49}}{dt} = k_{1r71}x_{46}x_{48} - k_{2r71}x_{49} - k_{1r73}x_{49}x_{51} + k_{2r73}x_{107} + k_{1r76}x_{108} \quad (\text{O.49})$$

$$\frac{dx_{50}}{dt} = -k_{1r72}x_{46}x_{50} + k_{2r72}x_{51} \quad (\text{O.50})$$

$$\frac{dx_{51}}{dt} = k_{1r72}x_{46}x_{50} - k_{2r72}x_{51} - k_{1r73}x_{49}x_{51} + k_{2r73}x_{107} + k_{1r74}x_{107} \quad (\text{O.51})$$

$$\frac{dx_{52}}{dt} = k_{1r74}x_{107} - k_{1r75}x_{52}x_{53} + k_{2r75}x_{108} - k_{1r77}x_{52}x_{75} + k_{2r77}x_{109} + k_{1r80}x_{110} \quad (\text{O.52})$$

$$\frac{dx_{53}}{dt} = -k_{1r75}x_{52}x_{53} + k_{2r75}x_{108} + k_{1r76}x_{108} \quad (\text{O.53})$$

$$\begin{aligned} \frac{dx_{54}}{dt} = & -k_{1r46}x_{29}x_{54} + k_{2r46}x_{96} + k_{1r47}x_{96} + k_{1r78}x_{109} - k_{1r79}x_{54}x_{55} + k_{2r79}x_{110} + \\ & + k_{1r89}x_{57}x_{54} + k_{2r89}x_{115} + k_{1r90}x_{115} - k_{1r92}x_{59}x_{54} + k_{2r92}x_{116} + k_{1r93}x_{116} + \\ & - k_{1r98}x_{61}x_{54} + k_{2r98}x_{118} + k_{1r99}x_{118} - k_{1r123}x_{78}x_{54} + k_{2r123}x_{127} + k_{1r124}x_{127} \end{aligned} \quad (\text{O.54})$$

$$\frac{dx_{55}}{dt} = -k_{1r79}x_{54}x_{55} + k_{2r79}x_{110} + k_{1r80}x_{110} \quad (\text{O.55})$$

$$\frac{dx_{56}}{dt} = -k_{1r81}x_{56}x_{59} + k_{2r81}x_{111} - k_{1r83}x_{56}x_{62} + k_{2r83}x_{112} + k_{1r86}x_{113} + k_{1r88}x_{114} \quad (\text{O.56})$$

$$\begin{aligned} \frac{dx_{57}}{dt} = & k_{1r82}x_{111} + k_{1r84}x_{112} - k_{1r85}x_{57}x_{68} + k_{2r85}x_{113} - k_{1r87}x_{57}x_{41} + \\ & + k_{2r87}x_{114} - k_{1r89}x_{57}x_{54} + k_{2r89}x_{115} + k_{1r91}x_{58} - k_{1r108}x_{69}x_{57} + \\ & + k_{2r108}x_{121} + k_{1r109}x_{121} \end{aligned} \quad (\text{O.57})$$

$$\frac{dx_{58}}{dt} = k_{1r90}x_{115} - k_{1r91}x_{58} \quad (\text{O.58})$$

$$\frac{dx_{59}}{dt} = -k_{1r81}x_{56}x_{59} + k_{2r81}x_{111} + k_{1r82}x_{111} - k_{1r92}x_{59}x_{54} + k_{2r92}x_{116} + k_{1r94}x_{60} \quad (\text{O.59})$$

$$\frac{dx_{60}}{dt} = k_{1r93}x_{116} - k_{1r94}x_{60} \quad (\text{O.60})$$

$$\frac{dx_{61}}{dt} = -k_{1r95}x_{61}x_{63} + k_{2r95}x_{117} + k_{1r97}x_{62} - k_{1r98}x_{61}x_{54} + k_{2r98}x_{118} + k_{1r100}x_{64} \quad (\text{O.61})$$

$$\frac{dx_{62}}{dt} = -k_{1r83}x_{56}x_{62} + k_{2r83}x_{112} + k_{1r84}x_{112} + k_{1r96}x_{117} - k_{1r97}x_{62} \quad (\text{O.62})$$

$$\frac{dx_{63}}{dt} = -k_{1r95}x_{61}x_{63} + k_{2r95}x_{117} + k_{1r96}x_{117} \quad (\text{O.63})$$

$$\frac{dx_{64}}{dt} = k_{1r99}x_{118} - k_{1r100}x_{64} \quad (\text{O.64})$$

$$\frac{dx_{65}}{dt} = -k_{1r101}x_{39}x_{65} + k_{2r101}x_{66} + k_{1r104}x_{67} \quad (\text{O.65})$$

$$\frac{dx_{66}}{dt} = k_{1r101}x_{39}x_{65} - k_{2r101}x_{66} - k_{1r102}x_{66}x_{38} + k_{2r102}x_{119} \quad (\text{O.66})$$

$$\frac{dx_{67}}{dt} = k_{1r103}x_{119} - k_{1r104}x_{67} - k_{1r105}x_{67}x_{41} + k_{2r105}x_{120} + k_{1r107}x_{68} \quad (\text{O.67})$$

$$\frac{dx_{68}}{dt} = -k_{1r85}x_{57}x_{68} + k_{2r85}x_{113} + k_{1r86}x_{113} + k_{1r106}x_{120} - k_{1r107}x_{68} \quad (\text{O.68})$$

$$\frac{dx_{69}}{dt} = -k_{1r108}x_{69}x_{57} + k_{2r108}x_{121} + k_{1r110}x_{70} - k_{1r111}x_{71}x_{69} + k_{2r111}x_{122} + k_{1r112}x_{122} \quad (\text{O.69})$$

$$\frac{dx_{70}}{dt} = k_{1r109}x_{121} - k_{1r110}x_{70} \quad (\text{O.70})$$

$$\frac{dx_{71}}{dt} = -k_{1r111}x_{71}x_{69} + k_{2r111}x_{122} + k_{1r113}x_{72} \quad (\text{O.71})$$

$$\frac{dx_{72}}{dt} = k_{1r112}x_{122} - k_{1r113}x_{72} - k_{1r114}x_{72}x_{73} + k_{2r114}x_{74} \quad (\text{O.72})$$

$$\frac{dx_{73}}{dt} = -k_{1r114}x_{72}x_{73} + k_{2r114}x_{74} \quad (\text{O.73})$$

$$\begin{aligned} \frac{dx_{74}}{dt} = & k_{1r114}x_{72}x_{73} - k_{2r114}x_{74} - k_{1r117}x_{76}x_{74} + k_{2r117}x_{124} + k_{1r118}x_{124} + \\ & - k_{1r121}x_{78}x_{74} + k_{2r121}x_{126} + k_{1r122}x_{126} \end{aligned} \quad (\text{O.74})$$

$$\frac{dx_{75}}{dt} = -k_{1r77}x_{52}x_{75} + k_{2r77}x_{109} + k_{1r78}x_{109} \quad (\text{O.75})$$

$$\frac{dx_{76}}{dt} = -k_{1r115}x_{76}x_{41} + k_{2r115}x_{123} - k_{1r117}x_{76}x_{74} + k_{2r117}x_{124} + k_{1r120}x_{125} \quad (\text{O.76})$$

$$\frac{dx_{77}}{dt} = -k_{1r35}x_{14}x_{77} + k_{2r35}x_{91} + k_{1r36}x_{91} + k_{1r116}x_{123} + k_{1r118}x_{124} - k_{1r119}x_{77}x_{78} + k_{2r119}x_{125} \quad (\text{O.77})$$

$$\begin{aligned} \frac{dx_{78}}{dt} = & -k_{1r119}x_{77}x_{78} + k_{2r119}x_{125} + k_{1r120}x_{125} - k_{1r121}x_{78}x_{74} + k_{2r121}x_{126} + \\ & -k_{1r123}x_{78}x_{54} + k_{2r123}x_{127} + k_{1r125}x_{79} \end{aligned} \quad (\text{O.78})$$

$$\frac{dx_{79}}{dt} = k_{1r122}x_{126} + k_{1r124}x_{127} - k_{1r125}x_{79} \quad (\text{O.79})$$

$$\frac{dx_{80}}{dt} = k_{1r2}x_3^2 - k_{2r2}x_{80} - k_{1r3}x_{80} \quad (\text{O.80})$$

$$\frac{dx_{81}}{dt} = k_{1r6}x_6x_8 - k_{2r6}x_{81} - k_{1r7}x_{81} \quad (\text{O.81})$$

$$\frac{dx_{82}}{dt} = k_{1r10}x_{10}^2 - k_{2r10}x_{82} - k_{1r11}x_{82} \quad (\text{O.82})$$

$$\frac{dx_{83}}{dt} = k_{1r13}x_{12}x_{13} - k_{2r13}x_{83} - k_{1r14}x_{83} \quad (\text{O.83})$$

$$\frac{dx_{84}}{dt} = k_{1r16}x_{15}^2 - k_{2r16}x_{84} - k_{1r17}x_{84} \quad (\text{O.84})$$

$$\frac{dx_{85}}{dt} = k_{1r19}x_{17}x_{18} - k_{2r19}x_{85} - k_{1r20}x_{85} \quad (\text{O.85})$$

$$\frac{dx_{86}}{dt} = k_{1r25}x_{25}x_{22} - k_{2r25}x_{86} - k_{1r26}x_{86} \quad (\text{O.86})$$

$$\frac{dx_{87}}{dt} = k_{1r27}x_{25}x_{23} - k_{2r27}x_{87} - k_{1r28}x_{87} \quad (\text{O.87})$$

$$\frac{dx_{88}}{dt} = k_{1r29}x_{25}x_{24} - k_{2r29}x_{88} - k_{1r30}x_{88} \quad (\text{O.88})$$

$$\frac{dx_{89}}{dt} = k_{1r31}x_{26}x_{27} - k_{2r31}x_{89} - k_{1r32}x_{89} \quad (\text{O.89})$$

$$\frac{dx_{90}}{dt} = k_{1r33}x_{14}x_{41} - k_{2r33}x_{90} - k_{1r34}x_{90} \quad (\text{O.90})$$

$$\frac{dx_{91}}{dt} = k_{1r35}x_{14}x_{77} - k_{2r35}x_{91} - k_{1r36}x_{91} \quad (\text{O.91})$$

$$\frac{dx_{92}}{dt} = k_{1r38}x_{29}x_{32} - k_{2r38}x_{92} - k_{1r39}x_{92} \quad (\text{O.92})$$

$$\frac{dx_{93}}{dt} = k_{1r40}x_{30}x_{41} - k_{2r40}x_{93} - k_{1r41}x_{93} \quad (\text{O.93})$$

$$\frac{dx_{94}}{dt} = k_{1r42}x_{30}x_{33} - k_{2r42}x_{94} - k_{1r43}x_{94} \quad (\text{O.94})$$

$$\frac{dx_{95}}{dt} = k_{1r44}x_{31}x_{33} - k_{2r44}x_{95} - k_{1r45}x_{95} \quad (\text{O.95})$$

$$\frac{dx_{96}}{dt} = k_{1r46}x_{29}x_{54} - k_{2r46}x_{96} - k_{1r47}x_{96} \quad (\text{O.96})$$

$$\frac{dx_{97}}{dt} = k_{1r50}x_{36}x_{35} - k_{2r50}x_{97} - k_{1r51}x_{97} \quad (\text{O.97})$$

$$\frac{dx_{98}}{dt} = k_{1r52}x_{37}x_{35} - k_{2r52}x_{98} - k_{1r53}x_{98} \quad (\text{O.98})$$

$$\frac{dx_{99}}{dt} = k_{1r54}x_{37}x_{33} - k_{2r54}x_{99} - k_{1r55}x_{99} \quad (\text{O.99})$$

$$\frac{dx_{100}}{dt} = k_{1r56}x_{38}x_{33} - k_{2r56}x_{100} - k_{1r57}x_{100} \quad (\text{O.100})$$

$$\frac{dx_{101}}{dt} = k_{1r58}x_{39}x_{38} - k_{2r58}x_{101} - k_{1r59}x_{101} \quad (\text{O.101})$$

$$\frac{dx_{102}}{dt} = k_{1r60}x_{40}x_{38} - k_{2r60}x_{102} - k_{1r61}x_{102} \quad (\text{O.102})$$

$$\frac{dx_{103}}{dt} = k_{1r62}x_{40}x_{42} - k_{2r62}x_{103} - k_{1r63}x_{103} \quad (\text{O.103})$$

$$\frac{dx_{104}}{dt} = k_{1r64}x_{41}x_{42} - k_{2r64}x_{104} - k_{1r65}x_{104} \quad (\text{O.104})$$

$$\frac{dx_{105}}{dt} = k_{1r67}x_{45}x_{44} - k_{2r67}x_{105} - k_{1r68}x_{105} \quad (\text{O.105})$$

$$\frac{dx_{106}}{dt} = k_{1r69}x_{46}x_{47} - k_{2r69}x_{106} - k_{1r70}x_{106} \quad (\text{O.106})$$

$$\frac{dx_{107}}{dt} = k_{1r73}x_{49}x_{51} - k_{2r73}x_{107} - k_{1r74}x_{107} \quad (\text{O.107})$$

$$\frac{dx_{108}}{dt} = k_{1r75}x_{52}x_{53} - k_{2r75}x_{108} - k_{1r76}x_{108} \quad (\text{O.108})$$

$$\frac{dx_{109}}{dt} = k_{1r77}x_{52}x_{75} - k_{2r77}x_{109} - k_{1r78}x_{109} \quad (\text{O.109})$$

$$\frac{dx_{110}}{dt} = k_{1r79}x_{54}x_{55} - k_{2r79}x_{110} - k_{1r80}x_{110} \quad (\text{O.110})$$

$$\frac{dx_{111}}{dt} = k_{1r81}x_{56}x_{59} - k_{2r81}x_{111} - k_{1r82}x_{111} \quad (\text{O.111})$$

$$\frac{dx_{112}}{dt} = k_{1r83}x_{56}x_{62} - k_{2r83}x_{112} - k_{1r84}x_{112} \quad (\text{O.112})$$

$$\frac{dx_{113}}{dt} = k_{1r85}x_{57}x_{68} - k_{2r85}x_{113} - k_{1r86}x_{113} \quad (\text{O.113})$$

$$\frac{dx_{114}}{dt} = k_{1r87}x_{57}x_{41} - k_{2r87}x_{114} - k_{1r88}x_{114} \quad (\text{O.114})$$

$$\frac{dx_{115}}{dt} = k_{1r89}x_{57}x_{54} - k_{2r89}x_{115} - k_{1r90}x_{115} \quad (\text{O.115})$$

$$\frac{dx_{116}}{dt} = k_{1r92}x_{59}x_{54} - k_{2r92}x_{116} - k_{1r93}x_{116} \quad (\text{O.116})$$

$$\frac{dx_{117}}{dt} = k_{1r95}x_{61}x_{63} - k_{2r95}x_{117} - k_{1r96}x_{117} \quad (\text{O.117})$$

$$\frac{dx_{118}}{dt} = k_{1r98}x_{61}x_{54} - k_{2r98}x_{118} - k_{1r99}x_{118} \quad (\text{O.118})$$

$$\frac{dx_{119}}{dt} = k_{1r102}x_{66}x_{38} - k_{2r102}x_{119} - k_{1r103}x_{119} \quad (\text{O.119})$$

$$\frac{dx_{120}}{dt} = k_{1r105}x_{67}x_{41} - k_{2r105}x_{120} - k_{1r106}x_{120} \quad (\text{O.120})$$

$$\frac{dx_{121}}{dt} = k_{1r108}x_{69}x_{57} - k_{2r108}x_{121} - k_{1r109}x_{121} \quad (\text{O.121})$$

$$\frac{dx_{122}}{dt} = k_{1r111}x_{71}x_{69} - k_{2r111}x_{122} - k_{1r112}x_{122} \quad (\text{O.122})$$

$$\frac{dx_{123}}{dt} = k_{1r115}x_{76}x_{41} - k_{2r115}x_{123} - k_{1r116}x_{123} \quad (\text{O.123})$$

$$\frac{dx_{124}}{dt} = k_{1r117}x_{76}x_{74} - k_{2r117}x_{124} - k_{1r118}x_{124} \quad (\text{O.124})$$

$$\frac{dx_{125}}{dt} = k_{1r119}x_{77}x_{78} - k_{2r119}x_{125} - k_{1r120}x_{125} \quad (\text{O.125})$$

$$\frac{dx_{126}}{dt} = k_{1r121}x_{78}x_{74} - k_{2r121}x_{126} - k_{1r122}x_{126} \quad (\text{O.126})$$

$$\frac{dx_{127}}{dt} = k_{1r123}x_{78}x_{54} - k_{2r123}x_{127} - k_{1r124}x_{127} \quad (\text{O.127})$$

We used Copasi (17) to implement the original model and export it as an SBML file

(Supplemental File S6 “original model.pdf”).

Supplemental Material S2. Computational Procedures

PSO. In each simulation, the number of particles comprising the swarm was set to 20 to compromise between computational efficiency and an accurate search for a solution. The inertia factor ω in equations 3 is critical for PSO convergence (18). A large inertia may significantly change the values of the model parameters to be inferred and facilitate the search for better solutions in unexplored areas of the parameter space (global exploration). In contrast, small inertia promotes local search of the parameter space and fine-tuning of solutions in explored areas. The inertia factor ω was therefore adaptively changed between the values of 1.1 and 0.1 to trade for global and local searches. As adaptive criteria, we selected the following scheme: 1) ω was initialized to 1.1 and a counter was initialized to 0; 2) the counter was increased by one unit if no improvement was made in the search or decreased by one unit if improvement was made in the search; 3) if the counter was smaller than 3, ω was multiplied by 2 to favorite global search; 4) if the counter was larger than 5, ω was divided by 2 to favorite local search; and 5) if ω exceeded the minimum or maximum values, it was reset to 1.1 or 0.1, respectively. The coefficient of self-recognition c_1 and the coefficient of the social component c_2 in equations 3 are not critical for PSO convergence. These coefficients are weights that fine-tune the decision of each particle to explore new areas of the space solutions following the memory of its own best position (c_1) and the experience of the most successful particle in the swarm (c_2). c_1 and c_2 were set to the values of 1.49, as in (18). To reduce the likelihood of particles getting trapped in the local minima, we implemented the lbest PSO (18) and adaptively varied the number of neighbor particles (m) influencing adjacent members in the swarm. As adaptive criterion, we selected the following scheme: 1) m was initially set to its minimum number of four randomly selected particles; 2) if no improvement was made in the search, m was increased by four randomly

selected particles; 3) if the search yielded improvement, m was reset to its minimum value of four randomly selected particles; and 4) if m exceeded the maximum value of particles in the swarm, m was set to 20 randomly selected particles.

Integrating mass-action modeling with PSO. We complemented mass-action modeling with PSO searching schemes to train the models against experimental data and design testable intervention strategies to inhibit aberrant cell signaling. The computational efficiency of our integrative approach strongly depends on the range of values for the unknown model parameters. Larger parameter spaces may improve the accuracy of model fitting; however, larger spaces may lead to time-scale separation between the dynamics of signaling molecules. Time-scale separation is representative of stiff systems and requires smaller time steps for convergence of the ODE solver. Computational time and model fitting accuracy can be significantly improved by supervising the choice of model parameters. We used hybrid strategies that combined supervised and unsupervised selections of model parameters to improve performance.

We structured our computational procedure as a five-step algorithm, implemented in Matlab (R2008b, The MathWorks, Natick, MA).

Step 1: Swarm particles (i.e., unknown model parameters) were randomly initialized within appropriately chosen intervals of values. The ranges for the model unknowns were selected by combining hybrid supervised and unsupervised approaches.

Step 2: The mass-action ODE model was solved using the implicit ode15s routine for stiff systems. This step comprised two stages. In the serum starvation stage, the concentration of the IGF-1 ligand was set to 0, and the ODE model was pre-run to compute the stationary levels attained by the proteins. We used these levels as the controls to normalize the protein profiles

computed during IGF-1 stimulation. In the stimulation stage, cells were stimulated with 75 ng/mL IGF-1 ligand, and the normalized model was trained against the normalized experimental data.

Step 3: The SD-weighted square error (SqE) was computed according to equation 4 in quick guide to equations and assumptions.

Step 4: Particle positions and velocities were updated according to equations 3 in quick guide to equations and assumptions.

Step 5: Steps 2-4 were repeated until SqE was lower than an arbitrary tolerance ($\text{tol}=10^{-4}$) or the maximum number of iterations (2500) was exceeded.

Integrating mass-action modeling with random sampling of model parameters. Mass-action modeling was complemented with a random sampling of model parameters to identify combined perturbations of targeted molecules and inhibit aberrant cell signaling. We structured our computational procedure as a four-step algorithm, implemented in Matlab (R2008b, The MathWorks, Natick, MA).

Step 1: Unknown model parameters (i.e., multiple targeted perturbations) were randomly sampled within intervals of values that had been selected by combining hybrid supervised and unsupervised approaches.

Step 2: The mass-action ODE model was solved using the implicit ode15s routine for stiff systems. This step comprised two stages. In the serum starvation stage, the concentration of the IGF-1 ligand was set to 0, and the ODE model was pre-run to compute the stationary levels attained by the proteins. These levels were used as the controls to normalize the protein profiles computed during IGF-1 stimulation. In the stimulation stage, cells were stimulated with 75

ng/mL IGF-1 ligand, and the normalized levels of p-AKT, p-MAPK, and p-p70S6K were computed.

Step 3: We stored the collections of model parameters (multiple targeted perturbations), generating levels of p-AKT, p-MAPK, and p-p70S6K that were decreased by at least five-fold compared with those measured in aberrant MDA-MB231 cells.

Step 4: Steps 1-3 were repeated until 200 collections of model parameters (multiple targeted perturbations) were identified.

Ranking identified targeted perturbations. Optimal combinations of targeted inhibitors were identified by comparing the model parameters inferred from the aberrant signaling measured in the MDA-MB231 cell line with randomly sampled collections of parameters (i.e., multiple targeted perturbations) that could restore user-defined signaling changes. The most influential kinetic rates and protein concentrations were ranked using the median deviation (MD) and standard deviation (SD) of the identified candidate targets, as proposed by Yang et al (19). We defined the MD as the distance between the levels of candidate targets in the aberrant and user-defined networks; therefore, MD represented how influential the identified targets were. A negative MD suggested inhibition of the candidate target, whereas a positive MD indicated activation. The SD provided an index of the consistency with which candidate targets were scored as influential. A small SD was representative of high consistency, and a large SD indicated low consistency. Targeted perturbations were then ranked by computing the absolute value of the ratio of MD to SD. The larger this ratio was, the more effective the target perturbation was at inhibiting aberrant cell signaling. To obtain reliable results, we used the procedure to identify 200 collections of relevant targets (listed in the Supplemental File S3

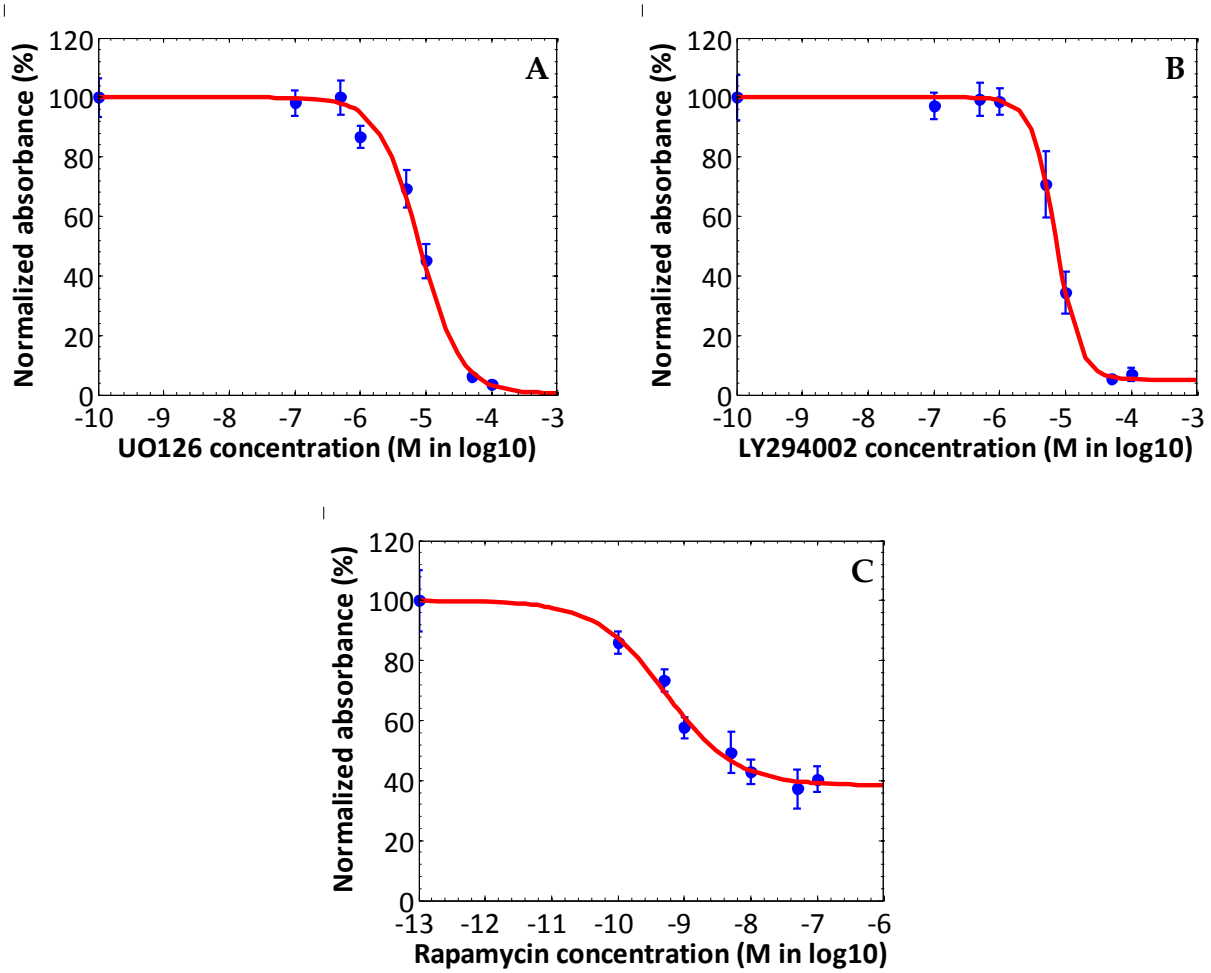
“combinatorial inhibition.xls”) for three different sets of model parameters that fell into the region of acceptable fitting (Supplemental File S2 “three parameter sets.xls”). If n represents the total number of model parameters and m represents the total number of collections of candidate targets identified by the procedure, the SD and MD of the i th parameter in the j th collection were computed as follows:

$$SD\ k_i = \sqrt{\frac{\sum_{j=1}^m k_{ij} - \bar{k}_i}{m-1}} \quad (S1)$$

$$MD(k_i) = \text{median } k_{i1}, \dots, k_{ij}, \dots, k_{im} - k_i^{aber}$$

In equation S1, $\bar{k}_i = \frac{1}{m} \sum_{j=1}^m k_{ij}$ represents the mean of the i th candidate target, and k_i^{aber} represents the corresponding parameter inferred from aberrant signaling in MDA-MB231 cells.

Supplemental Material S3. Dose response of the MDA-MB231 cell line to treatment with drug inhibitors.

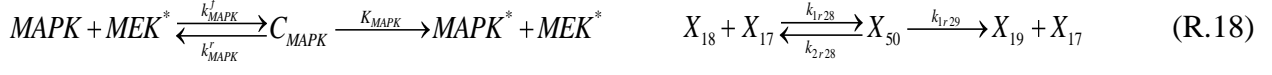
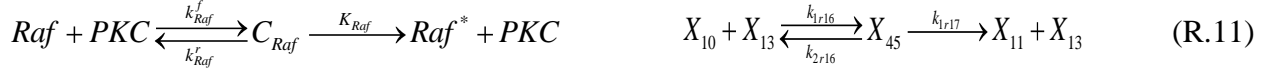


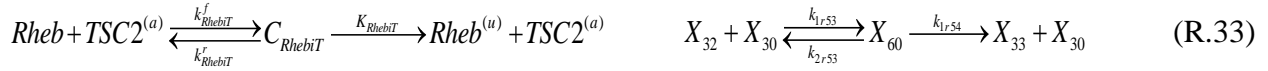
Supplemental Figure 2: Dose response of MDA-MB231 cells to treatment with different inhibitors. (A) UO126; (B) LY294002; (C) rapamycin. Solid circle and error bars represent the means and standard deviations of normalized absorbance measured using crystal violet assays. Solid lines denote the theoretical dose response computed using Microsoft GraphPad Prism (Redmont, WA).

Supplemental Material S4. Reduced IGFR signaling network in the MDA-MB231 breast cancer cell line.

Implementing mass-action models comprising several coupled ODEs and many unknown parameters may limit the computational efficiency of the ODE solver. Faster implementation of large mass-action models can instead be achieved through model reduction, which allows a decreased number of coupled ODEs and unknown parameters. Focusing our attention on the most relevant species in the IGFR signaling network, we reduced the 77 chemical reactions to a subset of 41, as follows:







Reactions 1-2 describe IGFR phosphorylation, and reactions 3-4 model IRS-1 activation.

Reactions 5-7 account for negative feedback regulation mediated by MAPK and p70S6K.

Reactions 8-10 and 13-19 model MAPK activation through the Ras-Raf-MEK cascade, reactions

13-14 account for AKT-mediated inhibition of Raf, and reactions 20-23 describe IRS-mediated

activation and PTEN-mediated inhibition of AKT. Reactions 24-27 account for inhibition of

AMPK and GSK3 by AKT, and reactions 28-32 model activation and inhibition of TSC2.

Finally, reactions 33-35 model Rheb-mediated mTOR activation, and reactions 36-41 describe

MAPK-, mTOR-, and AKT-mediated activation of p70S6K.

The original model was thus reduced to 65 coupled ODEs and 161 model unknowns, 96 of which were signaling rate constants and the remaining 65 of which were initial concentrations:

$$dx_1/dt = -k_{1r1}x_1x_2 + k_{2r1}x_3 \quad (\text{R.1})$$

$$dx_2/dt = -k_{1r1}x_1x_2 + k_{2r1}x_3 \quad (\text{R.2})$$

$$dx_3/dt = k_{1r1}x_1x_2 - k_{2r1}x_3 - k_{1r2}x_3 + k_{2r2}x_4 - k_{1r3}x_5x_3 + k_{2r3}x_{40} + k_{1r4}x_{40} + \\ - k_{1r11}x_8x_3 + k_{2r11}x_{43} + k_{1r12}x_{43} \quad (\text{R.3})$$

$$dx_4/dt = k_{1r2}x_3 - k_{2r2}x_4 \quad (\text{R.4})$$

$$dx_5/dt = -k_{1r3}x_5x_3 + k_{2r3}x_{40} + k_{1r5}x_6 - k_{1r6}x_5x_{19} + k_{2r6}x_{41} - k_{1r8}x_5x_{37} + k_{2r8}x_{42} + k_{1r10}x_7 \quad (\text{R.5})$$

$$dx_6/dt = k_{1r4}x_{40} - k_{1r5}x_6 - k_{1r13}x_8x_6 + k_{2r13}x_{44} + k_{1r14}x_{44} - k_{1r32}x_{21}x_6 + k_{2r32}x_{52} + k_{1r33}x_{52} \quad (\text{R.6})$$

$$dx_7/dt = k_{1r7}x_{41} + k_{1r9}x_{42} - k_{1r10}x_7 \quad (\text{R.7})$$

$$dx_8/dt = -k_{1r11}x_8x_3 + k_{2r11}x_{43} - k_{1r13}x_8x_6 + k_{2r13}x_{44} + k_{1r15}x_9 \quad (\text{R.8})$$

$$dx_9/dt = k_{1r12}x_{43} + k_{1r14}x_{44} - k_{1r15}x_9 - k_{1r23}x_9x_{11} + k_{2r23}x_{15} \quad (\text{R.9})$$

$$dx_{10}/dt = -k_{1r16}x_{10}x_{13} + k_{2r16}x_{45} + k_{1r19}x_{46} - k_{1r20}x_{10}x_{22} + k_{2r20}x_{47} + k_{1r22}x_{12} \quad (\text{R.10})$$

$$dx_{11}/dt = k_{1r17}x_{45} - k_{1r18}x_{11}x_{14} + k_{2r18}x_{46} - k_{1r23}x_9x_{11} + k_{2r23}x_{15} \quad (\text{R.11})$$

$$dx_{12}/dt = k_{1r21}x_{47} - k_{1r22}x_{12} \quad (\text{R.12})$$

$$dx_{13}/dt = -k_{1r16}x_{10}x_{13} + k_{2r16}x_{45} + k_{1r17}x_{45} \quad (\text{R.13})$$

$$dx_{14}/dt = -k_{1r18}x_{11}x_{14} + k_{2r18}x_{46} + k_{1r19}x_{46} - k_{1r26}x_{17}x_{14} + k_{2r26}x_{49} + k_{1r27}x_{49} \quad (\text{R.14})$$

$$dx_{15}/dt = k_{1r23}x_9x_{11} - k_{2r23}x_{15} - k_{1r24}x_{16}x_{15} + k_{2r24}x_{48} + k_{1r25}x_{48} \quad (\text{R.15})$$

$$dx_{16}/dt = -k_{1r24}x_{16}x_{15} - k_{2r24}x_{48} + k_{1r27}x_{49} \quad (\text{R.16})$$

$$dx_{17}/dt = k_{1r25}x_{48} - k_{1r26}x_{17}x_{14} + k_{2r26}x_{49} - k_{1r28}x_{18}x_{17} + k_{2r28}x_{50} + k_{1r29}x_{50} \quad (\text{R.17})$$

$$dx_{18}/dt = -k_{1r28}x_{18}x_{17} + k_{2r28}x_{50} + k_{1r31}x_{51} \quad (\text{R.18})$$

$$dx_{19}/dt = -k_{1r6}x_5x_{19} + k_{2r6}x_{41} + k_{1r7}x_{41} + k_{1r29}x_{50} - k_{1r30}x_{19}x_{20} + k_{2r30}x_{51} + \\ -k_{1r48}x_{30}x_{19} + k_{2r48}x_{58} + k_{1r49}x_{58} - k_{1r57}x_{36}x_{19} + k_{2r57}x_{61} + k_{1r58}x_{61} \quad (\text{R.19})$$

$$dx_{20}/dt = -k_{1r30}x_{19}x_{20} + k_{2r30}x_{51} + k_{1r31}x_{51} \quad (\text{R.20})$$

$$dx_{21}/dt = -k_{1r32}x_{21}x_6 + k_{2r32}x_{52} + k_{1r34}x_{22} - k_{1r35}x_{21}x_{24} + k_{2r35}x_{53} + k_{1r37}x_{23} \quad (\text{R.21})$$

$$dx_{22}/dt = -k_{1r20}x_{10}x_{22} + k_{2r20}x_{47} + k_{1r21}x_{47} + k_{1r33}x_{52} - k_{1r34}x_{22} - k_{1r38}x_{25}x_{22} + \\ + k_{2r38}x_{54} + k_{1r39}x_{54} - k_{1r41}x_{27}x_{22} + k_{2r41}x_{55} + k_{1r42}x_{55} - k_{1r50}x_{30}x_{22} + \\ + k_{2r50}x_{59} + k_{1r51}x_{59} - k_{1r65}x_{38}x_{22} + k_{2r65}x_{65} + k_{1r66}x_{65} \quad (\text{R.22})$$

$$dx_{23}/dt = k_{1r36}x_{53} - k_{1r37}x_{23} \quad (\text{R.23})$$

$$dx_{24}/dt = -k_{1r35}x_{21}x_{24} + k_{2r35}x_{53} + k_{1r36}x_{53} \quad (\text{R.24})$$

$$dx_{25}/dt = -k_{1r38}x_{25}x_{22} + k_{2r38}x_{54} + k_{1r40}x_{26} - k_{1r44}x_{29}x_{25} + k_{2r44}x_{56} + k_{1r45}x_{56} \quad (\text{R.25})$$

$$dx_{26}/dt = k_{1r39}x_{54} - k_{1r40}x_{26} \quad (\text{R.26})$$

$$dx_{27}/dt = -k_{1r41}x_{27}x_{22} + k_{2r41}x_{55} + k_{1r43}x_{28} - k_{1r46}x_{29}x_{27} + k_{2r46}x_{57} + k_{1r47}x_{57} \quad (\text{R.27})$$

$$dx_{28}/dt = k_{1r42}x_{55} - k_{1r43}x_{28} \quad (\text{R.28})$$

$$dx_{29}/dt = -k_{1r44}x_{29}x_{25} + k_{2r44}x_{56} - k_{1r46}x_{29}x_{27} + k_{2r46}x_{57} + k_{1r49}x_{58} \quad (\text{R.29})$$

$$dx_{30}/dt = k_{1r45}x_{56} + k_{1r47}x_{57} - k_{1r48}x_{30}x_{19} + k_{2r48}x_{58} - k_{1r50}x_{30}x_{22} + k_{2r50}x_{59} + k_{1r52}x_{31} - k_{1r53}x_{32}x_{30} + k_{2r53}x_{60} + k_{1r54}x_{60} \quad (\text{R.30})$$

$$dx_{31}/dt = k_{1r51}x_{59} - k_{1r52}x_{31} \quad (\text{R.31})$$

$$dx_{32}/dt = -k_{1r53}x_{32}x_{30} + k_{2r53}x_{60} + k_{1r55}x_{33} - k_{1r56}x_{34}x_{32} + k_{2r56}x_{35} \quad (\text{R.32})$$

$$dx_{33}/dt = k_{1r54}x_{60} - k_{1r55}x_{33} \quad (\text{R.33})$$

$$dx_{34}/dt = -k_{1r56}x_{34}x_{32} + k_{2r56}x_{35} \quad (\text{R.34})$$

$$dx_{35}/dt = k_{1r56}x_{34}x_{32} - k_{2r56}x_{35} - k_{1r59}x_{36}x_{35} + k_{2r59}x_{62} + k_{1r60}x_{62} - k_{1r63}x_{38}x_{35} + k_{2r63}x_{64} + k_{1r64}x_{64} \quad (\text{R.35})$$

$$dx_{36}/dt = -k_{1r57}x_{36}x_{19} + k_{2r57}x_{61} - k_{1r59}x_{36}x_{35} + k_{2r59}x_{62} + k_{1r62}x_{63} \quad (\text{R.36})$$

$$dx_{37}/dt = -k_{1r8}x_5x_{37} + k_{2r8}x_{42} + k_{1r9}x_{42} + k_{1r58}x_{61} + k_{1r60}x_{62} - k_{1r61}x_{37}x_{38} + k_{2r61}x_{63} \quad (\text{R.37})$$

$$dx_{38}/dt = -k_{1r61}x_{37}x_{38} + k_{2r61}x_{63} + k_{1r62}x_{63} - k_{1r63}x_{38}x_{35} + k_{2r63}x_{64} + k_{1r65}x_{38}x_{22} + k_{2r65}x_{65} + k_{1r67}x_{39} \quad (\text{R.38})$$

$$dx_{39}/dt = k_{1r64}x_{64} + k_{1r66}x_{65} - k_{1r67}x_{39} \quad (\text{R.39})$$

$$dx_{40}/dt = k_{1r3}x_5x_3 - k_{2r3}x_{40} - k_{1r4}x_{40} \quad (\text{R.40})$$

$$dx_{41}/dt = k_{1r6}x_5x_{19} - k_{2r6}x_{41} - k_{1r7}x_{41} \quad (\text{R.41})$$

$$dx_{42}/dt = k_{1r8}x_5x_{37} - k_{2r8}x_{42} - k_{1r9}x_{42} \quad (\text{R.42})$$

$$dx_{43}/dt = k_{1r11}x_8x_3 - k_{2r11}x_{43} - k_{1r12}x_{43} \quad (\text{R.43})$$

$$dx_{44}/dt = k_{1r13}x_8x_6 - k_{2r13}x_{44} - k_{1r14}x_{44} \quad (\text{R.44})$$

$$dx_{45}/dt = k_{1r16}x_{10}x_{13} - k_{2r16}x_{45} - k_{1r17}x_{45} \quad (\text{R.45})$$

$$dx_{46}/dt = k_{1r18}x_{11}x_{14} - k_{2r18}x_{46} - k_{1r19}x_{46} \quad (\text{R.46})$$

$$dx_{47}/dt = k_{1r20}x_{10}x_{22} - k_{2r20}x_{47} - k_{1r21}x_{47} \quad (\text{R.47})$$

$$dx_{48}/dt = k_{1r24}x_{16}x_{15} - k_{2r24}x_{48} - k_{1r25}x_{48} \quad (\text{R.48})$$

$$dx_{49}/dt = k_{1r26}x_{17}x_{14} - k_{2r26}x_{49} - k_{1r27}x_{49} \quad (\text{R.49})$$

$$dx_{50}/dt = k_{1r28}x_{18}x_{17} - k_{2r28}x_{50} - k_{1r29}x_{50} \quad (\text{R.50})$$

$$dx_{51}/dt = k_{1r30}x_{19}x_{20} - k_{2r30}x_{51} - k_{1r31}x_{51} \quad (\text{R.51})$$

$$dx_{52}/dt = k_{1r32}x_{21}x_6 - k_{2r32}x_{52} - k_{1r33}x_{52} \quad (\text{R.52})$$

$$dx_{53}/dt = k_{1r35}x_{21}x_{24} - k_{2r35}x_{53} - k_{1r36}x_{53} \quad (\text{R.53})$$

$$dx_{54}/dt = k_{1r38}x_{25}x_{22} - k_{2r38}x_{54} - k_{1r39}x_{54} \quad (\text{R.54})$$

$$dx_{55}/dt = k_{1r41}x_{27}x_{22} - k_{2r41}x_{55} - k_{1r42}x_{55} \quad (\text{R.55})$$

$$dx_{56}/dt = k_{1r44}x_{29}x_{25} - k_{2r44}x_{56} - k_{1r45}x_{56} \quad (\text{R.56})$$

$$dx_{57}/dt = k_{1r46}x_{29}x_{27} - k_{2r46}x_{57} - k_{1r47}x_{57} \quad (\text{R.57})$$

$$dx_{58}/dt = k_{1r48}x_{30}x_{19} - k_{2r48}x_{58} - k_{1r49}x_{58} \quad (\text{R.58})$$

$$dx_{59}/dt = k_{1r50}x_{30}x_{22} - k_{2r50}x_{59} - k_{1r51}x_{59} \quad (\text{R.59})$$

$$dx_{60}/dt = k_{1r53}x_{32}x_{30} - k_{2r53}x_{60} - k_{1r54}x_{60} \quad (\text{R.60})$$

$$dx_{61}/dt = k_{1r57}x_{36}x_{19} - k_{2r57}x_{61} - k_{1r58}x_{61} \quad (\text{R.61})$$

$$dx_{62}/dt = k_{1r59}x_{36}x_{35} - k_{2r59}x_{62} - k_{1r60}x_{62} \quad (\text{R.62})$$

$$dx_{63}/dt = k_{1r61}x_{37}x_{38} - k_{2r61}x_{63} - k_{1r62}x_{63} \quad (\text{R.63})$$

$$dx_{64}/dt = k_{1r63}x_{38}x_{35} - k_{2r63}x_{64} - k_{1r64}x_{64} \quad (\text{R.64})$$

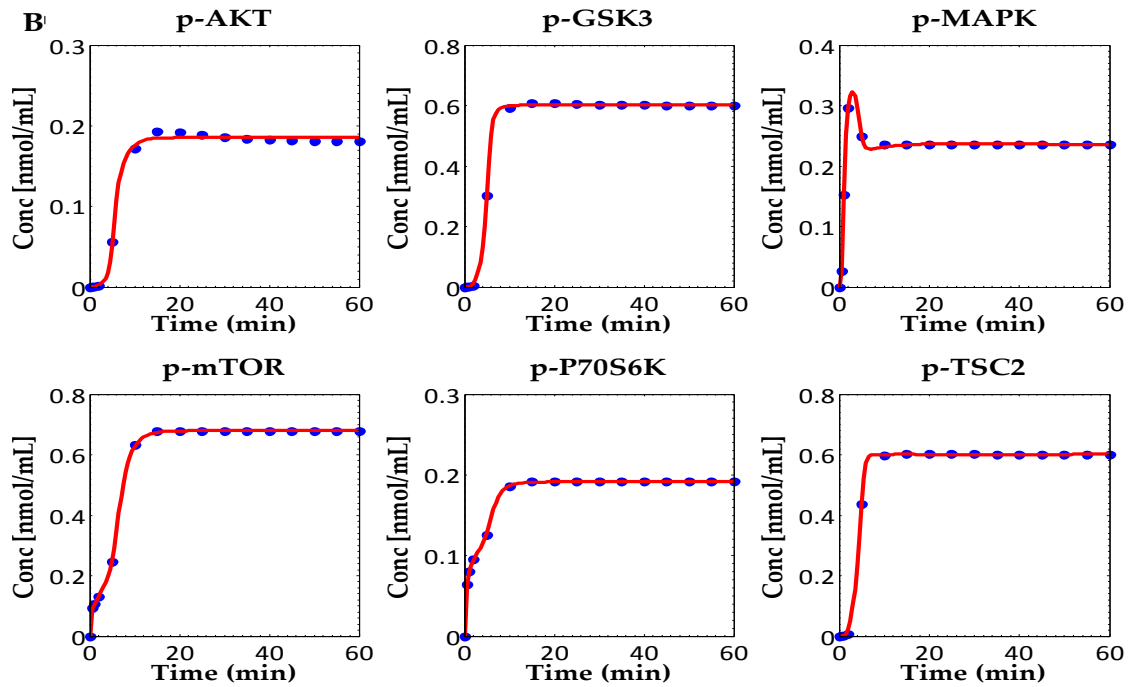
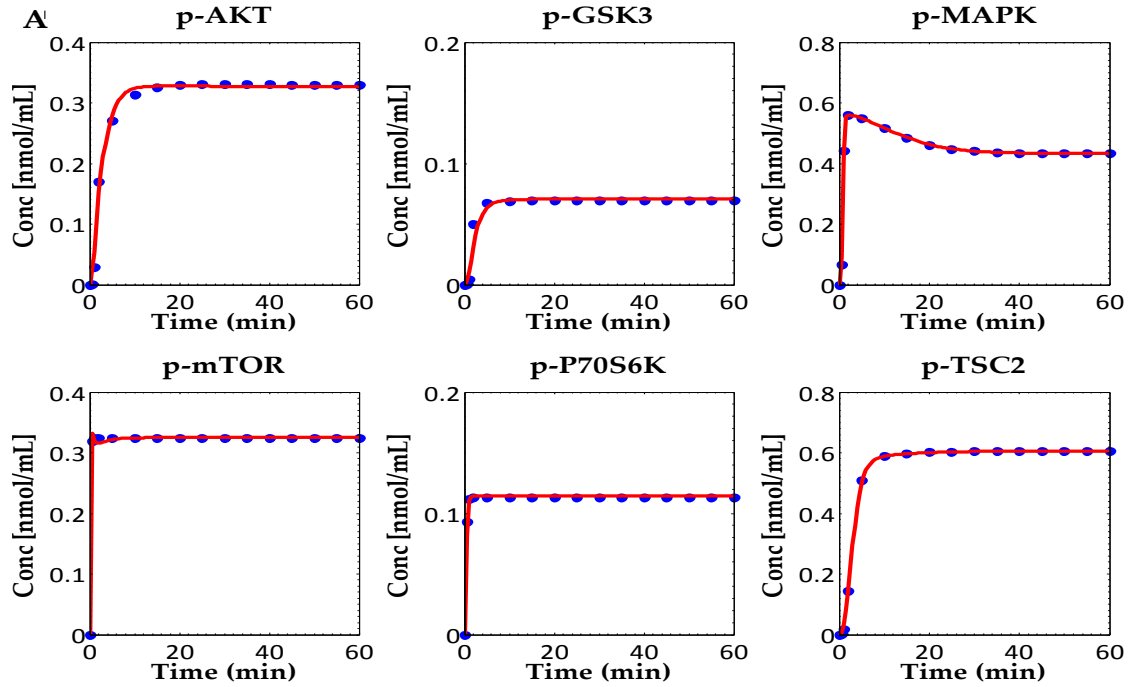
$$dx_{65}/dt = k_{1r65}x_{38}x_{22} - k_{2r65}x_{65} - k_{1r66}x_{65} \quad (\text{R.65})$$

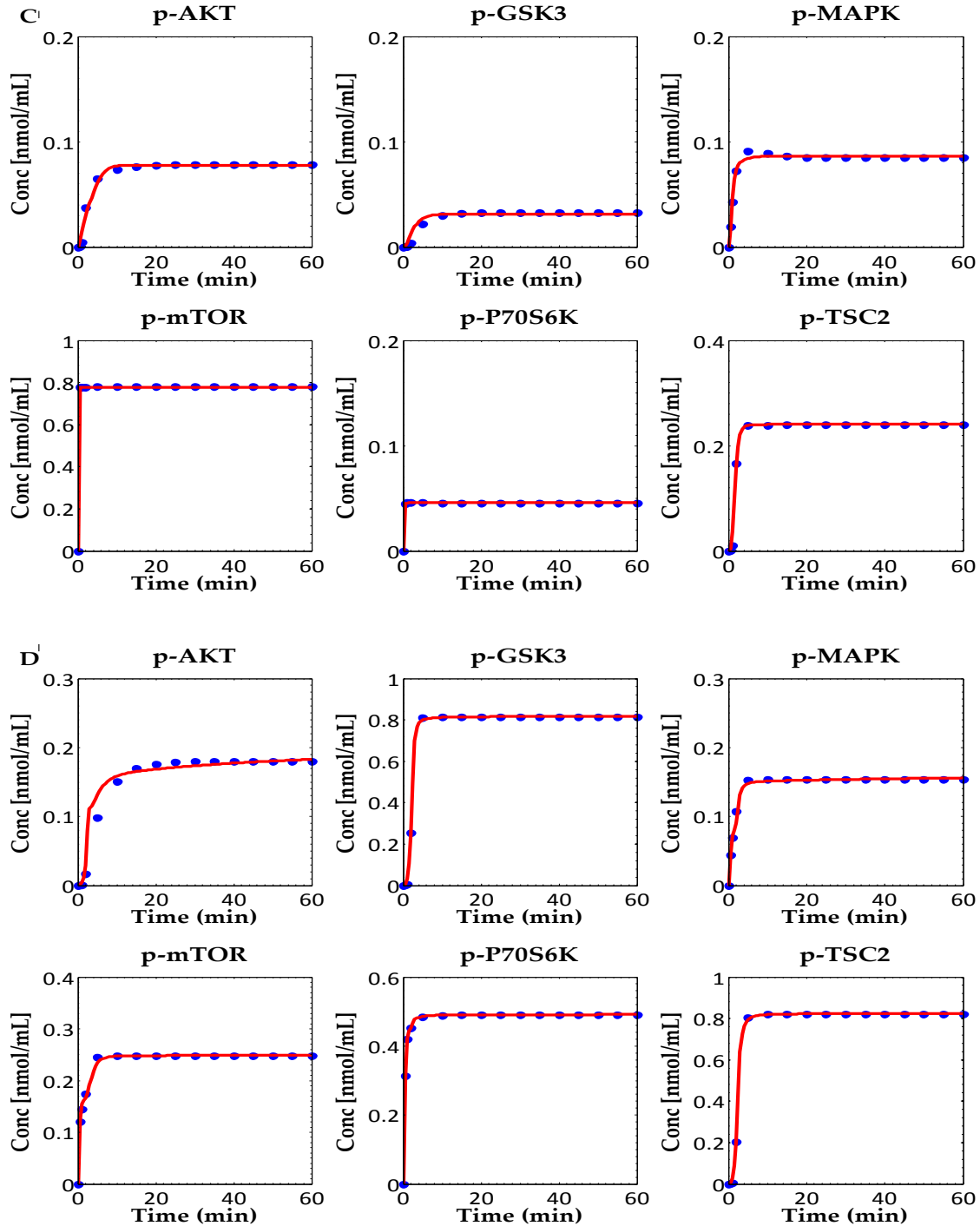
We used Copasi (17) to implement the reduced model and export it as an SBML file

(Supplemental File S7 “reduced model.pdf”).

Supplemental Material S5. Comparison between dynamics predicted by the original and reduced ODE models.

To determine whether the reduced model could adequately predict the dynamics of IGFR signaling in MDA-MB231 cells, we used the original model to predict changes in MAPK, AKT, GSK3, TSC2, mTOR, and p70S6K phosphorylation levels at various times for four randomly selected sets of parameters (listed in Supplemental File S4 “original model parameters.xls”). We then determined whether similar protein profiles could be predicted using the reduced model. We used particle swarm optimization (PSO) to fit the reduced model against the protein profiles obtained using the original model. The reduced model parameters inferred using PSO are listed in Supplemental File S5 “reduced model parameters.xls”. Supplemental Figure 3 shows the comparisons between the time courses of the proteins generated using the two models. Because the protein profiles predicted by the reduced model matched those generated by the original model for all sets of selected parameters, it is expected that the reduced model can provide a good enough representation of the biological system described by the original model and that both mass-action models would equally predict the dynamics of the IGFR signaling network in the MDA-MB231 cell line.

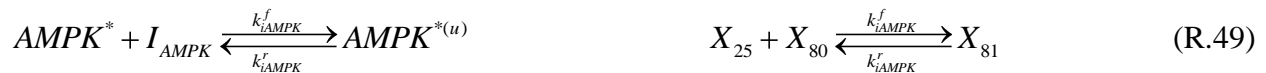
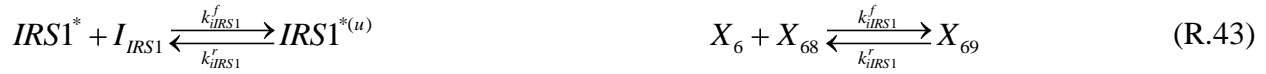




Supplemental Figure 3: Comparison between protein profiles predicted by the original and reduced mass-action models for four randomly selected sets of unknown parameters. Model parameters are listed in Supplemental Files S4 “original model parameters.xls” (OMset) and S5 “reduced model parameters.xls” (RMset). (A) OMset 1 and RMset 1, (B) OMset 2 and RMset 2, (C) OMset 3 and RMset 3, and (D) OMset 4 and RMset 4. Circles: levels of phosphorylated proteins generated by the original model at 0, 0.5, 1, 2, 5, 10, 15, 20, 25, 30, 25, 40, 45, 50, 55, or 60 minutes; solid lines: time courses of phosphorylated proteins predicted by the reduced model.

Supplemental Material S6. Perturbing IGFR signaling dynamics using drug inhibitors.

We used the trained mass-action model to predict the effect of single-targeted perturbation on the dynamics of IGFR signaling networks in the MDA-MB231 cell line. The mass-action model was augmented with the chemical reactions that described the simplified mechanism of drug inhibition. The U0126 MEK inhibitor competes with ATP for the ATP-binding site on MEK (20). Therefore, MEK inhibition does not affect the phosphorylation level of MEK but impairs the functional activity p-MEK to regulate its downstream effector, MAPK. The effect of drug inhibition on IGFR signaling dynamics was thus modeled under the assumption that inhibitors render their target molecules unavailable (superscript u) for functional activation and inhibition of downstream effectors:





Equations R.3, R.6, R.9, R.11, R.17, R.19, R.22, R.25, R.27, R.30, R.32, R.35, and R.37 were then rewritten as follows:

$$\begin{aligned} dx_3/dt = & k_{1r1}x_1x_2 - k_{2r1}x_3 - k_{1r2}x_3 + k_{2r2}x_4 - k_{1r3}x_5x_3 + k_{2r3}x_{40} + k_{1r4}x_{40} + \\ & - k_{1r11}x_8x_3 + k_{2r11}x_{43} + k_{1r12}x_{43} - k_{iIGFRf}x_3x_{66} + k_{iIGFRr}x_{67} \end{aligned} \quad (R.3)$$

$$\begin{aligned} dx_6/dt = & k_{1r4}x_{40} - k_{1r5}x_6 - k_{1r13}x_8x_6 + k_{2r13}x_{44} + k_{1r14}x_{44} - k_{1r32}x_{21}x_6 + \\ & + k_{2r32}x_{52} + k_{1r33}x_{52} - k_{iIRS1f}x_6x_{68} + k_{iIRS1r}x_{69} \end{aligned} \quad (R.6)$$

$$dx_9/dt = k_{1r12}x_{43} + k_{1r14}x_{44} - k_{1r15}x_9 - k_{1r23}x_9x_{11} + k_{2r23}x_{15} - k_{iRASf}x_9x_{70} + k_{iRASr}x_{71} \quad (R.9)$$

$$dx_{11}/dt = k_{1r17}x_{45} - k_{1r18}x_{11}x_{14} + k_{2r18}x_{46} - k_{1r23}x_9x_{11} + k_{2r23}x_{15} - k_{iRAFf}x_{11}x_{72} + k_{iRAFr}x_{73} \quad (R.11)$$

$$\begin{aligned} dx_{17}/dt = & k_{1r25}x_{48} - k_{1r26}x_{17}x_{14} + k_{2r26}x_{49} - k_{1r28}x_{18}x_{17} + k_{2r28}x_{50} + k_{1r29}x_{50} + \\ & - k_{iMEKf}x_{17}x_{74} + k_{iMEKr}x_{75} \end{aligned} \quad (R.17)$$

$$\begin{aligned} dx_{19}/dt = & -k_{1r6}x_5x_{19} + k_{2r6}x_{41} + k_{1r7}x_{41} + k_{1r29}x_{50} - k_{1r30}x_{19}x_{20} + k_{2r30}x_{51} + \\ & - k_{1r48}x_{30}x_{19} + k_{2r48}x_{58} + k_{1r49}x_{58} - k_{1r57}x_{36}x_{19} + k_{2r57}x_{61} + k_{1r58}x_{61} + \\ & - k_{iMAPKf}x_{19}x_{76} + k_{iMAPKr}x_{77} \end{aligned} \quad (R.19)$$

$$\begin{aligned} dx_{22}/dt = & -k_{1r20}x_{10}x_{22} + k_{2r20}x_{47} + k_{1r21}x_{47} + k_{1r33}x_{52} - k_{1r34}x_{22} - k_{1r38}x_{25}x_{22} + \\ & + k_{2r38}x_{54} + k_{1r39}x_{54} - k_{1r41}x_{27}x_{22} + k_{2r41}x_{55} + k_{1r42}x_{55} - k_{1r50}x_{30}x_{22} + \\ & + k_{2r50}x_{59} + k_{1r51}x_{59} - k_{1r65}x_{38}x_{22} + k_{2r65}x_{65} + k_{1r66}x_{65} - k_{iAKTf}x_{22}x_{78} + k_{iAKTr}x_{79} \end{aligned} \quad (R.22)$$

$$dx_{25}/dt = -k_{1r38}x_{25}x_{22} + k_{2r38}x_{54} + k_{1r40}x_{26} - k_{1r44}x_{29}x_{25} + k_{2r44}x_{56} + k_{1r45}x_{56} +$$

$$-k_{iAMPKf}x_{25}x_{80} + k_{iAMPKr}x_{81} \quad (\text{R.25})$$

$$dx_{27}/dt = -k_{1r41}x_{27}x_{22} + k_{2r41}x_{55} + k_{1r43}x_{28} - k_{1r46}x_{29}x_{27} + k_{2r46}x_{57} + k_{1r47}x_{57} +$$

$$-k_{iGSK3f}x_{27}x_{82} + k_{iGSK3r}x_{83} \quad (\text{R.27})$$

$$dx_{30}/dt = k_{1r45}x_{56} + k_{1r47}x_{57} - k_{1r48}x_{30}x_{19} + k_{2r48}x_{58} - k_{1r50}x_{30}x_{22} + k_{2r50}x_{59} +$$

$$+ k_{1r52}x_{31} - k_{1r53}x_{32}x_{30} + k_{2r53}x_{60} + k_{1r54}x_{60} - k_{iTSC2f}x_{30}x_{84} + k_{iTSC2r}x_{85} \quad (\text{R.30})$$

$$dx_{32}/dt = -k_{1r53}x_{32}x_{30} + k_{2r53}x_{60} + k_{1r55}x_{33} - k_{1r56}x_{34}x_{32} + k_{2r56}x_{35} +$$

$$-k_{iRheb f}x_{32}x_{86} + k_{iRhebr}x_{87} \quad (\text{R.32})$$

$$dx_{35}/dt = k_{1r56}x_{34}x_{32} - k_{2r56}x_{35} - k_{1r59}x_{36}x_{35} + k_{2r59}x_{62} + k_{1r60}x_{62} - k_{1r63}x_{38}x_{35} +$$

$$+ k_{2r63}x_{64} + k_{1r64}x_{64} - k_{imTORf}x_{35}x_{88} + k_{imTORr}x_{89} \quad (\text{R.35})$$

$$dx_{37}/dt = -k_{1r8}x_5x_{37} + k_{2r8}x_{42} + k_{1r9}x_{42} + k_{1r58}x_{61} + k_{1r60}x_{62} - k_{1r61}x_{37}x_{38} + k_{2r61}x_{63} +$$

$$-k_{ip70f}x_{37}x_{90} + k_{ip70r}x_{91} \quad (\text{R.37})$$

The following equations were also included in the model:

$$dx_{66}/dt = -k_{iIGFRf}x_3x_{66} + k_{iIGFRr}x_{67} \quad (\text{S.66})$$

$$dx_{67}/dt = k_{iIGFRf}x_3x_{66} - k_{iIGFRr}x_{67} \quad (\text{S.67})$$

$$dx_{68}/dt = -k_{iIRS1f}x_6x_{68} + k_{iIRS1r}x_{69} \quad (\text{S.68})$$

$$dx_{69}/dt = k_{iIRS1f}x_6x_{68} - k_{iIRS1r}x_{69} \quad (\text{S.69})$$

$$dx_{70}/dt = -k_{iRASf}x_9x_{70} + k_{iRASr}x_{71} \quad (\text{S.70})$$

$$dx_{71}/dt = k_{iRASf}x_9x_{70} - k_{iRASr}x_{71} \quad (\text{S.71})$$

$$dx_{72}/dt = -k_{iRAFf}x_{11}x_{72} + k_{iRAFr}x_{73} \quad (\text{S.72})$$

$$dx_{73}/dt = k_{iRAFf}x_{11}x_{72} - k_{iRAFr}x_{73} \quad (\text{S.73})$$

$$dx_{74}/dt = -k_{iMEKf}x_{17}x_{74} + k_{iMEKr}x_{75} \quad (\text{S.74})$$

$$dx_{75}/dt = k_{iMEKf}x_{17}x_{74} - k_{iMEKr}x_{75} \quad (\text{S.75})$$

$$dx_{76}/dt = -k_{iMAPKf}x_{19}x_{76} + k_{iMAPKr}x_{77} \quad (\text{S.76})$$

$$dx_{77}/dt = k_{iMAPKf}x_{19}x_{76} - k_{iMAPKr}x_{77} \quad (\text{S.77})$$

$$dx_{78}/dt = -k_{iAKTf}x_{22}x_{78} + k_{iAKTr}x_{79} \quad (\text{S.78})$$

$$dx_{79}/dt = k_{iAKTf}x_{22}x_{78} - k_{iAKTr}x_{79} \quad (\text{S.79})$$

$$dx_{80}/dt = -k_{iAMPKf}x_{25}x_{80} + k_{iAMPKr}x_{81} \quad (\text{S.80})$$

$$dx_{81}/dt = k_{iAMPKf}x_{25}x_{80} - k_{iAMPKr}x_{81} \quad (\text{S.81})$$

$$dx_{82}/dt = -k_{iGSK3f}x_{27}x_{82} + k_{iGSK3r}x_{83} \quad (\text{S.82})$$

$$dx_{83}/dt = k_{iGSK3f}x_{27}x_{82} - k_{iGSK3r}x_{83} \quad (\text{S.83})$$

$$dx_{84}/dt = -k_{iTSC2f}x_{30}x_{84} + k_{iTSC2r}x_{85} \quad (\text{S.84})$$

$$dx_{85}/dt = k_{iTSC2f}x_{30}x_{84} - k_{iTSC2r}x_{85} \quad (\text{S.85})$$

$$dx_{86}/dt = -k_{iRheb}x_{32}x_{86} + k_{iRhebr}x_{87} \quad (\text{S.86})$$

$$dx_{87}/dt = k_{iRheb}x_{32}x_{86} - k_{iRhebr}x_{87} \quad (\text{S.87})$$

$$dx_{88}/dt = -k_{imTORf}x_{35}x_{88} + k_{imTORr}x_{89} \quad (\text{S.88})$$

$$dx_{89}/dt = k_{imTORf}x_{35}x_{88} - k_{imTORr}x_{89} \quad (\text{S.89})$$

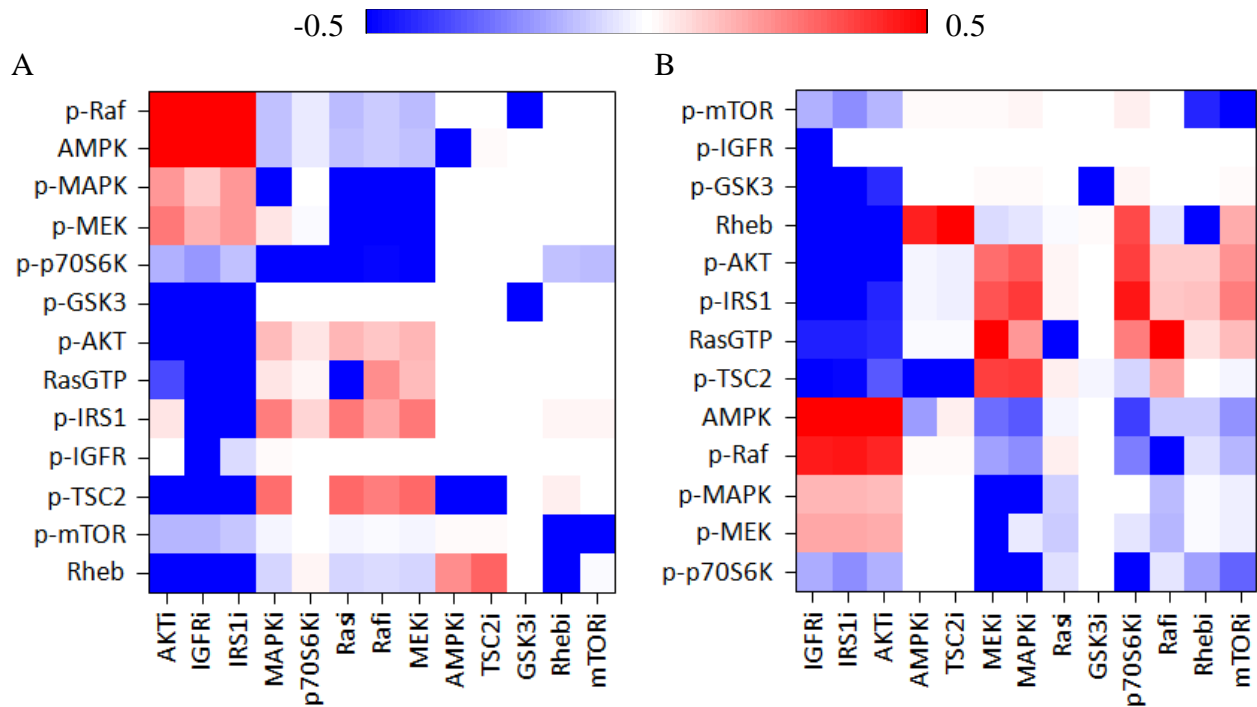
$$dx_{90}/dt = -k_{ip70S6f}x_{37}x_{90} + k_{ip70S6r}x_{91} \quad (\text{S.90})$$

$$dx_{91}/dt = k_{ip70S6f}x_{37}x_{90} - k_{ip70S6r}x_{91} \quad (\text{S.91})$$

The initial concentration of U0126, LY294002, and rapamycin were set to be equal to the drug inhibitor concentrations experimentally used (10 μ M, 50 μ M, and 50 nM, respectively). The concentrations of the other drug inhibitors were arbitrarily set at 10 μ M. The signaling rate

constants of the forward reactions in equations R.66-R.91 were at least one order of magnitude larger than the corresponding rates of reverse reactions to ensure proper inhibition.

Using the augmented, trained mass-action model, we predicted differential levels of proteins in single-inhibited versus noninhibited MDA-MB231 cells after 2 hours of stimulation with 75 ng/mL IGF-1 for sets of parameters that generated protein time courses that fell into the region of acceptable fitting (listed in Supplemental File S2 “three parameter sets.xls”), as shown in Supplemental Figure 4.



Supplemental Figure 4: The effect of single-molecule inhibition of IGFR network. Differential levels of proteins in single-molecule-inhibited versus noninhibited MDA-MB231 cells after 2 hours of stimulation with 75 ng/mL IGF-1 were predicted using the trained mass-action model. Numerical values were converted into \log_{10} . The blue color represents inhibition, white denotes no variation in protein levels, and red indicates activation. To obtain reliable results, the analysis was repeated for three sets of parameters that generate protein time courses that fall into the region of acceptable fitting (listed in the Supplemental File S2 “three parameter sets.xls”). (A) set2; (B) set3. The computational results obtained using set1 are shown in Figure 3 in the manuscript.

Supplemental Files.

Supplemental File S1. The supplemental file “fitting variability.xls” includes 10 collections of model parameters that generated protein profiles that equally fit the time course data experimentally measured on RPPA.

Supplemental File S2. The supplemental file “three parameter sets.xls” includes three sets of model parameters that generated protein profiles that equally fit the time course data experimentally measured on RPPA. These sets were randomly selected out of the 10 sets listed in Supplemental File S1 and used to computationally predict, in triplicate, the effect of individual and combined inhibition of targeted molecule on IGFR signaling network dynamics.

Supplemental File S3. The supplemental file “combinatorial inhibition.xls” includes 200 collections of combinatorial targeted perturbations that restored user-defined signaling outputs in the MDA-MB231 cell line for the sets listed in the Supplemental File S2 “three parameter sets.xls”.

Supplemental File S4. The supplemental file “original model parameters.xls” includes four sets of randomly selected model parameters that were used to implement the original model (equations O1-O127) and generate time courses of biologically relevant proteins involved in the IGFR signaling network.

Supplemental File S5. The supplemental file “reduced model parameters.xls” includes four sets of model parameters that were used to implement the reduced model (equations R1-R65) and

generate protein profiles that matched those obtained using the original model.

Supplemental Files S6 and S7. The supplemental file, “original model.pdf”, and supplemental file, “reduced model.pdf”, contain the SBML versions of the original and reduced models, respectively.

Supplemental Tables

Table IA

Rank	Parameter	MD	ABS (MD)/SD	Target
1	K_{IRSd}	0.05386	2.11339	p-IRS1 inhibition
2	k_{MEKd}^f	20.21719	1.98482	p-MEK inhibition
3	k_{MAPKd}^f	18.32918	1.80587	p-MAPK inhibition
4	$k_{IGFRint}^f$	1.98527	1.69548	p-IGFR inhibition
5	K_{AKTd}	20.82549	1.68417	p-AKT inhibition
6	k_{IRSiS}^f	11.65082	1.6453	p-IRS1 inhibition
7	k_{TSC2aG}^f	18.55147	1.57861	TSC2 activation

Table IB

Rank	Parameter	MD	ABS (MD)/SD	Target
1	K_{IRSd}	1.49508	2.67577	p-IRS1 inhibition
2	k_{MAPKd}^f	20.67875	2.13757	p-MAPK inhibition
3	K_{AKTd}	19.6798	1.96492	p-AKT inhibition
4	k_{MEKd}^f	16.1026	1.90236	p-MEK inhibition
5	$k_{IGFRint}^f$	0.07026	1.8582	p-IGFR inhibition
6	K_{RasRaf}^r	1.52808	1.68929	p-Ras:Raf inhibition
7	K_{Rasd}	0.71527	1.61712	p-Ras inhibition

Table IC

Rank	Parameter	MD	ABS (MD)/SD	Target
1	K_{IRSd}	0.08931	2.57739	p-IRS inhibition
2	k_{MEKd}^f	21.71343	2.24431	p-MEK inhibition
3	K_{AKTd}	23.53143	2.08157	p-AKT inhibition
4	k_{MAPKd}^f	13.66176	2.03733	p-MAPK inhibition
5	$k_{IGFRint}^f$	0.5879	1.64959	p-IGFR inhibition
6	k_{S6KaT}^f	0.00001	1.64346	p-p70S6K activation
7	K_{S6Pra}	0.08079	1.51858	p-p70S6K inhibition

Supplemental Table I. The effect of combined inhibition on IGFR signaling network. Influential targets ranked according to the ABS (MD/SD) using sets of model parameters (targeted perturbations) that generate protein time courses that fall into the region of acceptable fitting (listed in the Supplemental File S2 “three parameter sets.xls”). Abbreviations: ABS = absolute value; MD = median deviation; SD = standard deviation. Table IA: set 1; Table IB: set2; Table IC: set3.

Table IIA

	5 minutes			60 minutes	
	<i>Experimental data</i>	<i>Modeling predictions</i>		<i>Experimental data</i>	<i>Modeling predictions</i>
p-AKT	↓	↓	p-AKT	↓	↓
p-GSK3	↓	↓	p-GSK3	↓	↓
p-MAPK	↓	↓	p-MAPK	↓	↓
p-mTOR	↓	↓	p-mTOR	↓	↓
p-p70S6K	↓	↓	p-p70S6K	↓	↓
p-TSC2	↓	↓	p-TSC2	↓	↓

Table IIB

	5 minutes			60 minutes	
	<i>Experimental data</i>	<i>Modeling predictions</i>		<i>Experimental data</i>	<i>Modeling predictions</i>
p-AKT	↑	↑	p-AKT	↑	↑
p-GSK3	↑	↑	p-GSK3	↑	↑
p-MAPK	↓	↓	p-MAPK	↓	↓
p-mTOR	↓	↓	p-mTOR	↓	↓
p-p70S6K	↓	↓	p-p70S6K	↓	↓
p-TSC2	↑	↑	p-TSC2	↑	↑

Supplemental Table II: Qualitative comparison between measured and predicted differential levels of phosphorylated proteins in MDA-MB231 cells simulated with 75 ng/mL IGF-1 for 5 minutes or 60 minutes in the absence of inhibition and after 1 hour of incubation with MEK and PI3K (Table IIA) or with MEK and mTOR inhibitors (Table IIB).

Table III					
	Initial random seeding	Set 1	Set2	Set3	Set4
		Error	Error	Error	Error
PSO	Run 1	0.001935	0.004549	0.000603	0.001002
	Run 2	0.001644	0.001017	0.000597	0.000249
	Run 3	0.002058	0.006531	0.001512	0.001630
GA	Run 1	10.4339	1.28127	0.925727	0.0268329
	Run 2	5.83392	1.23666	0.925727	0.0199196
	Run 3	8.85885	9.88149	0.925727	0.332285
SA	Run 1	0.365486	1.03858	0.0756718	0.417092
	Run 2	0.693289	0.867789	0.121014	0.452542
	Run 3	0.579803	1.25373	0.131323	0.339764

Supplemental Table III. Comparison between performance of particle swarm optimization (PSO), genetic algorithm (GA), and simulated annealing (SA) in training the reduced mass-action model against time courses of proteins generated using the original mass-action model for the sets of parameters listed in Supplemental File S4 “original model parameters.xls”. Simulations were performed using Copasi (17) and repeated three times with different random seeds of the reduced model unknown parameters. PSO was implemented using the following parameters for the Copasi solver—iteration limit: 2000, swarm size: 20, standard deviation: 1e-6, random generator: 1, and seed: 0. GA was implemented using the following parameters for the Copasi solver—number of generations: 2000, population size: 20, and random number generator: 1. SA was implemented using the following parameters for the Copasi solver—start temperature: 1, cooling factor: 0.85, tolerance: 1e-6, random generator: 1, and seed: 0. PSO, GA, and SA were run for at least 40,000 number of function evaluations. The error was computed by setting the weight ω equal to 1 for all protein time courses (see Copasi experimental data window).

References

1. Ullrich A, Schlessinger J. Signal transduction by receptors with tyrosine kinase activity. *Cell* 1990; 61: 203-12.
2. Schlessinger J. Cell signaling by receptor tyrosine kinases. *Cell* 2000; 103: 211-25.
3. Manning BD, Cantley LC. AKT/PKB signaling: navigating downstream. *Cell* 2007; 129: 1261-74.
4. Easton JB, Kurmasheva RT, Houghton PJ. IRS-1: auditing the effectiveness of mTOR inhibitors. *Cancer Cell* 2006; 9: 153-5.
5. Vastrik I, D'Eustachio P, Schmidt E, et al. Reactome: a knowledge base of biologic pathways and processes. *Genome Biol* 2007; 8: R39.
6. Mirzoeva OK, Das D, Heiser LM, et al. Basal subtype and MAPK/ERK kinase (MEK)-phosphoinositide 3-kinase feedback signaling determine susceptibility of breast cancer cells to MEK inhibition. *Cancer Res* 2009; 69: 565-72.
7. Bhalla US, Iyengar R. Emergent properties of networks of biological signaling pathways. *Science* 1999; 283: 381-7.
8. Zimmermann S, Moelling K. Phosphorylation and regulation of Raf by Akt (protein kinase B). *Science* 1999; 286: 1741-4.
9. Inoki K, Ouyang H, Zhu T, et al. TSC2 integrates Wnt and energy signals via a coordinated phosphorylation by AMPK and GSK3 to regulate cell growth. *Cell* 2006; 126: 955-68.
10. Ma L, Teruya-Feldstein J, Bonner P, et al. Identification of S664 TSC2 phosphorylation as a marker for extracellular signal-regulated kinase mediated mTOR activation in tuberous sclerosis and human cancer. *Cancer Res* 2007; 67: 7106-12.

11. Carriere A, Cargnello M, Julien LA, et al. Oncogenic MAPK signaling stimulates mTORC1 activity by promoting RSK-mediated raptor phosphorylation. *Curr Biol* 2008; 18: 1269-77.
12. Hahn-Windgassen A, Nogueira V, Chen CC, Skeen JE, Sonenberg N, Hay N. Akt activates the mammalian target of rapamycin by regulating cellular ATP level and AMPK activity. *J Biol Chem* 2005; 280: 32081-9.
13. Ballif BA, Roux PP, Gerber SA, MacKeigan JP, Blenis J, Gygi SP. Quantitative phosphorylation profiling of the ERK/p90 ribosomal S6 kinase-signaling cassette and its targets, the tuberous sclerosis tumor suppressors. *Proc Natl Acad Sci U S A* 2005; 102: 667-72.
14. Lehman JA, Gomez-Cambronero J. Molecular crosstalk between p70S6k and MAPK cell signaling pathways. *Biochem Biophys Res Commun* 2002; 293: 463-9.
15. Hay N, Sonenberg N. Upstream and downstream of mTOR. *Genes Dev* 2004; 18: 1926-45.
16. Pullen N, Dennis PB, Andjelkovic M, et al. Phosphorylation and activation of p70s6k by PDK1. *Science* 1998; 279: 707-10.
17. Hoops S, Sahle S, Gauges R, et al. COPASI--a COMplex PATHway SIMulator. *Bioinformatics* 2006; 22: 3067-74.
18. Abraham A, Guo H, Liu H. Swarm intelligence: foundations, perspectives and applications. In: Nedjah N, de Macedo Mourelle L, editors. *Studies in computational intelligence*: Springer; 2006. p. 2-25.
19. Yang K, Bai H, Ouyang Q, Lai L, Tang C. Finding multiple target optimal intervention in disease-related molecular network. *Mol Syst Biol* 2008; 4: 228.

20. Duncia JV, Santella JB, 3rd, Higley CA, et al. MEK inhibitors: the chemistry and biological activity of U0126, its analogs, and cyclization products. *Bioorg Med Chem Lett* 1998; 8: 2839-44.